



# CT-Informed Skull Osteology of *Palaeolagus haydeni* (Mammalia: Lagomorpha) and Its Bearing on the Reconstruction of the Early Lagomorph Body Plan

Andrzej S. Wolniewicz<sup>1†</sup> and Łucja Fostowicz-Frelik<sup>1,2,3\*†</sup>

<sup>1</sup> Department of Evolutionary Paleobiology, Institute of Paleobiology, Polish Academy of Sciences, Warsaw, Poland, <sup>2</sup> Key Laboratory of Vertebrate Evolution and Human Origins, Institute of Vertebrate Paleontology and Paleoanthropology, Chinese Academy of Sciences, Beijing, China, <sup>3</sup> Center for Excellence in Life and Paleoenvironment, Chinese Academy of Sciences, Beijing, China

## OPEN ACCESS

### Edited by:

K. Christopher Beard,  
University of Kansas, United States

### Reviewed by:

John Wible,  
Carnegie Museum of Natural History,  
United States

Omella C. Bertrand,  
University of Edinburgh,  
United Kingdom

### \*Correspondence:

Łucja Fostowicz-Frelik  
lfost@twarda.pan.pl

### †ORCID:

Andrzej S. Wolniewicz  
orcid.org/0000-0002-6336-8916

Łucja Fostowicz-Frelik  
orcid.org/0000-0002-1266-1178

### Specialty section:

This article was submitted to  
Paleontology,  
a section of the journal  
Frontiers in Ecology and Evolution

**Received:** 03 December 2020

**Accepted:** 25 January 2021

**Published:** 17 February 2021

### Citation:

Wolniewicz AS and  
Fostowicz-Frelik Ł (2021) CT-Informed  
Skull Osteology of *Palaeolagus  
haydeni* (Mammalia: Lagomorpha)  
and Its Bearing on the Reconstruction  
of the Early Lagomorph Body Plan.  
*Front. Ecol. Evol.* 9:634757.  
doi: 10.3389/fevo.2021.634757

Lagomorpha is a clade of herbivorous mammals nested within Euarchontoglires, one of the major placental groups represented today. It comprises two extant families with markedly different body plans: the long-eared and long-limbed Leporidae (hares and rabbits) and the short-eared and short-limbed Ochotonidae (pikas). These two lagomorph lineages diverged probably during the latest Eocene/early Oligocene, but it is unclear whether the last common ancestor of crown lagomorphs was more leporid- or more ochotonid-like in morphology. *Palaeolagus*, an early lagomorph dominant in western North America from the late Eocene to Oligocene is of particular importance for addressing this controversy. Here, we present new and comprehensive data on the cranial anatomy of *Palaeolagus haydeni*, the type species for the genus, based on micro-computed tomography ( $\mu$ CT). Our  $\mu$ CT data allow us to confirm, revise and score for the very first time the states of several leporid-like and ochotonid-like characters in the skull of *Palaeolagus*. This mixed cranial architecture differentiates *Palaeolagus* from the crown groups of Lagomorpha and supports its phylogenetic status as a stem taxon.

**Keywords:** skull, Lagomorpha, Leporidae, Ochotonidae, *Palaeolagus*, cranial base, micro-computed tomography

## INTRODUCTION

Lagomorpha is a highly conservative clade of Glires, known in the fossil record since the early Eocene (Li et al., 2007; Fostowicz-Frelik et al., 2015; Lopatin and Averianov, 2020). Nowadays, Lagomorpha comprise leporids (hares and rabbits) and ochotonids (pikas); both families differ considerably in their external morphology, especially in the limb length and proportions, and the

**Abbreviations:** AMNH, American Museum of Natural History, New York, NY, United States; FMNH, Field Museum of Natural History, Chicago, IL, United States; IBS (formerly ZBS), Institute of Mammal Research, Polish Academy of Sciences, Białowieża, Poland; ISEZ, Institute of Systematics and Evolution of Animals, Polish Academy of Sciences, Cracow, Poland; MCZ, Museum of Comparative Zoology, Harvard University, Cambridge, MA, United States; USNM, National Museum of Natural History, Smithsonian Institution, Washington D.C., United States; ZPAL, Institute of Paleobiology, Polish Academy of Sciences, Warsaw, Poland.

size and shape of the pinnae. These two families also show marked differences in the skull structure and dentition (e.g., Wible, 2007; Dawson, 2008; Fostowicz-Frelik and Meng, 2013; Wilson et al., 2016), some of them due to parallel evolution and frequent homoplasy (Fostowicz-Frelik and Meng, 2013; Fostowicz-Frelik, 2017).

Most of the Paleogene fossil record of Lagomorpha is represented by stem taxa (e.g., Fostowicz-Frelik, 2013; Fostowicz-Frelik and Meng, 2013; Fostowicz-Frelik et al., 2015), and the precise ancestry and the time of origination of the crown lagomorph lineages remains uncertain. *Palaeolagus*, a speciose genus of the Paleogene North American lagomorph seems to be of particular importance for addressing this conundrum. Although *Palaeolagus* was historically regarded as an early leporid (mostly based on its dental morphology), the most recent phylogenetic analyses have recovered it as a stem lagomorph, even if close to the crown taxa (e.g., Wible, 2007; Fostowicz-Frelik and Meng, 2013; Lopatin and Averianov, 2020; but see Asher et al., 2019).

Currently, *Palaeolagus* includes nine species and spans from the late Eocene through the earliest Miocene interval (Dawson, 1958, 2008). This work concerns the type species *Palaeolagus haydeni*, known from the Oligocene of the Great Plains (e.g., Wood, 1940; Dawson, 1958, 2008). *P. haydeni* was a ubiquitous and abundant species of the genus and is represented by numerous remains, including well-preserved skulls (Figures 1, 2) and postcranial skeletons from the fossiliferous sediments of the White River Formation (see Wood, 1940; Dawson, 1958). Its abundance in the fossil record may be compared to the broad prevalence of extant *Oryctolagus cuniculus*, which, however, is related to *Palaeolagus* only distantly. These features position *Palaeolagus* as one of the most important taxa for understanding early lagomorph morphology and evolution. Despite the availability of material, very few contributions deal with the cranial anatomy of *Palaeolagus* (see Troxell, 1921; Dice, 1933; Wood, 1940; Dawson, 1958). Moreover, these studies leave out the details of the base of the skull and the braincase, due to past technical limitations of studying the fossil material. Some detailed aspects of the cranial anatomy of *Palaeolagus* were provided by Wible (2007), but his observations were not supported with relevant drawings or photographs.

Here, we present new data on the cranial anatomy of *P. haydeni*, based on micro-computed tomography ( $\mu$ CT). Our anatomical observations provide information important for inferring the character states present in the probable last common ancestor of ochotonids and leporids. They will also be of great importance in phylogenetic studies focusing on resolving the relationships at the base of Lagomorpha in particular, and Glires in general.

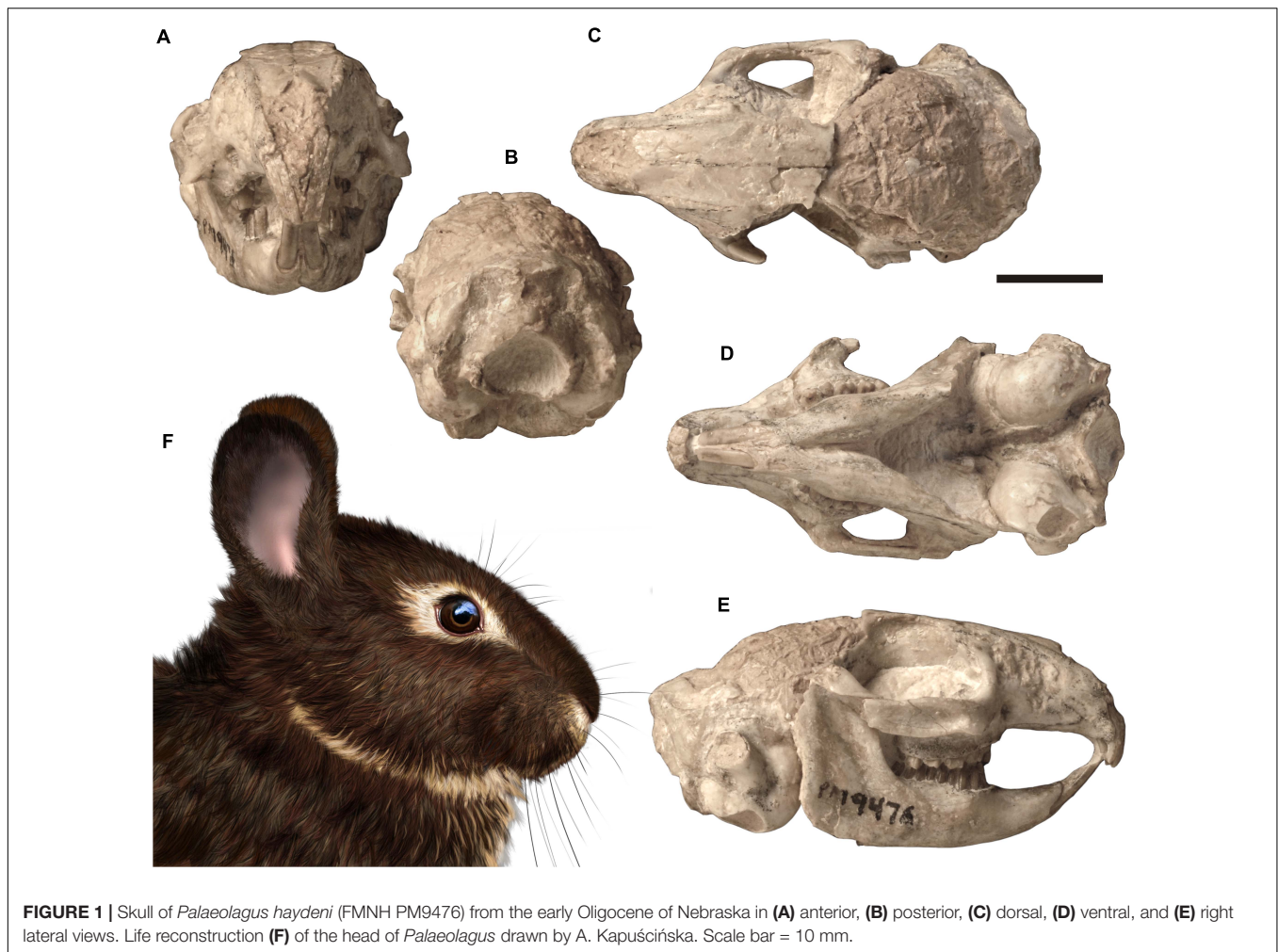
## MATERIALS AND METHODS

This study is based on CT-scan data from an almost complete cranium with mandible in occlusion of *Palaeolagus haydeni*

(FMNH PM9476) from the early Oligocene of the Brule Formation, Nebraska (Figures 1, 3). The skull roof is partially missing in this specimen (posterior frontals and parietals were lost during sedimentation), the anterior nasals and the left zygomatic arch are also largely damaged. To complement the study of the external cranial morphology, several partial skulls of *P. haydeni* were examined as comparative material: AMNH FM106111, a cranium with a slightly distorted muzzle and missing nasals; AMNH FM143956, an almost complete cranium with missing zygomatic arches (Figure 2); FMNH PM43030, an anterior part of a skull with a complete muzzle and orbit, associated with both anterior mandible bodies; MCZ 3373, a complete skull with both parts of the mandible *in situ* and partly missing parietals; USNM PAL 243590 and USNM 2530-49, both complete crania without mandibles, partly embedded in matrix. Additionally, we consulted the morphology of several extant lagomorphs (see Supplementary Material).

FMNH PM9476 was CT-scanned in a high-resolution Phoenix v|tome|x L 240 scanner (GE Measurement & Control Solutions) at the AMNH. The specimen was scanned in a single scan with the following parameters: voltage 170 kV, current 170  $\mu$ A and a 0.1 mm Cu filter to minimize beam hardening. The CT-data were reconstructed with Phoenix datos|x 2.0 software obtaining a total of 1401 images at a resolution of 0.0365 mm (isometric voxels). The reconstruction of the raw data generated a 16-bit TIFF image stack comprising 980 slices (570  $\times$  515 pixels). The original image stack was first uploaded into ImageJ 1.52a (Schneider et al., 2012) to remove beam hardening artifacts and increase the contrast between fossilized bone and rock matrix using the Brightness and Contrast tool (Image  $\rightarrow$  Adjust  $\rightarrow$  Brightness/Contrast). The adjusted images were then saved as an 8-bit TIFF image stack and uploaded into AvizoLite 2019.4 (Thermo Fischer Scientific 1995–2019) installed on a FUJITSU Celsius M740 workstation (processor: Intel Xeon CPU E5-2620 v4 2.10 GHz, RAM: 128 GB, graphics card: GeForce GTX 1050 Ti, hard drive: Samsung SSD 860 EVO 500 GB) operating on Windows 10 Pro (Microsoft 2019). Manual segmentation involved using the Lasso and Magic Wand tools. Because of extensive bone fusion, it was not possible to determine the position of sutures between: (1) the maxillae and the zygomatic bones; (2) the orbital portions of the frontals, the presphenoid, the orbitosphenoids, the alisphenoids, the pterygoids and the basisphenoid; and (3) the interparietal and supraoccipital. As a result, these bones were segmented not as individual elements, but as bone complexes, and the external sutures between them were inferred from observations of the external and internal surfaces of the 3D models, as well as from comparisons with additional specimens of *Palaeolagus* and extant lagomorphs. 3D models of individual bones and bone complexes were generated using the Unconstrained Smoothing option (smoothing extent = 2.5). Images of the 3D models were created using the Snapshot tool and compiled into figures using Adobe Photoshop Elements (Adobe 2020). The 3D models of FMNH PM9476 and digitally separated bones are available from the Dryad Digital Repository<sup>1</sup> (Fostowicz-Frelik and Wolniewicz, 2021).

<sup>1</sup><https://doi.org/10.5061/dryad.crjdfn338>



## Anatomical Terminology

The cranial anatomy of *P. haydeni* was described with reference to three previously published, comprehensive and well-illustrated accounts of extant lagomorph cranial anatomy: two historical descriptions of *Oryctolagus cuniculus* by Krause (1884) and Craigie (1948), and a more recent, comparative description of *Ochotona princeps* and *Romerolagus diazi* (Wible, 2007). The description of the cranial anatomy of the dog by Evans and de Lahunta (2013), a widely cited source for mammal anatomical nomenclature, was used as an additional reference. Because some of the anatomical structures were given markedly different names in all four studies (see **Supplementary Table 1**), for our description we decided to use the anatomical terms that were: (1) derived from English, rather than Latin [e.g., ‘nasoturbinate crest’ (Evans and de Lahunta, 2013) rather than ‘crista nasalis’ (Krause, 1884)]; (2) the least descriptive [e.g., ethmoidal fossa (Evans and de Lahunta, 2013) rather than ‘small pocket open posteriorly’ (Wible, 2007)]; and (3) anatomically most accurate [e.g., ‘apex of premaxillary process of nasal’ (this work) rather than ‘triangular process of nasal’ (Wible, 2007)]. We also avoided phrases taken from common language [e.g., ‘nasoturbinate crest’ rather than ‘nasoturbinal scroll’ (Craigie, 1948)]. In addition,

Wible and Shelley (2020) were consulted for nomenclature on the anatomy of the petrosal.

## OSTEOLOGICAL DESCRIPTION

### Nasal

The paired nasals form the dorsal surface of the rostrum and the roof of the nasal cavity. Their anterior margins also contribute to the dorsal margin of the external nasal aperture. In most specimens, including FMNH PM9476, only the posterior parts of the nasals are preserved, whereas their anterior portions are abraded due to their overall fragility (**Figures 3A–C,E, 4A–E**). However, the complete nasals can be observed in AMNH FM143956 (**Figures 2A–C**). Their general morphology does not depart from the description of Wood (1940, p. 279). Also, the anterior tips of the bones, not connected to the premaxillae, slightly narrow mediolaterally and protrude anterior to the incisors, overhanging the external nasal aperture.

The nasal is a dorsoventrally flattened bone that is much longer anteroposteriorly than it is wide mediolaterally. It forms a premaxillary process, laterally, and a frontal process, posteriorly.

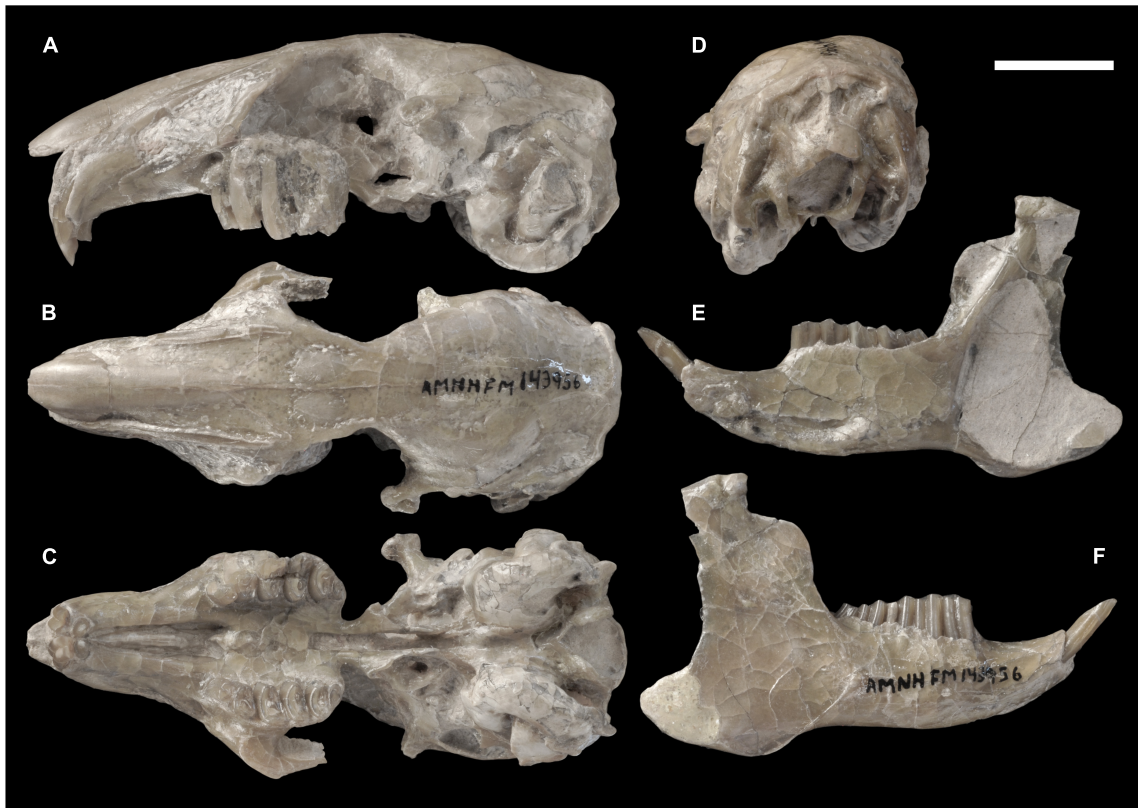


**FIGURE 2** | Skull of *Palaeolagus haydeni* (AMNH FM143956) from the early Oligocene of Wyoming in (A) left lateral, (B) dorsal, (C) ventral, and (D) posterior views. Mandible of the same specimen in (E) medial and (F) lateral views. Note the well-preserved nasal region and the completely preserved mandible. Scale bar = 10 mm.

The mediolateral width of the nasal increases posteriorly along its anteroposterior length, until the nasal attains its greatest mediolateral width at the base of the frontal process. This is similar to the condition present in extant leporids, but differs from *Ochotona*, in which the mediolateral width of the nasal decreases posteriorly or remains approximately constant throughout its entire anteroposterior length (Wible, 2007, char. 1; Fostowicz-Freluk et al., 2010). The dorsal surfaces of the preserved portions of the nasals in FMNH PM9476 are slightly concave throughout most of their anteroposterior length, but their orientation becomes sub-horizontal at the base of the frontal process. At the lateral border of the dorsal surface of each nasal a field of neurovascular foramina is present, arranged along the nasal process of the premaxilla (AMNH FM143956; **Figure 2A**). Our observations stand in opposition to those of Wood (1940, p. 279), who stated that *Palaeolagus* does not have any nutritive foramina located on the nasals, which are usually observed in extant leporids. Furthermore, Wood (1940, p. 279) considered it a primitive feature, similar to the state observed in *Ochotona*. According to our observations, the vascularization of the nasals was present in all studied *Palaeolagus* specimens that preserve the anterior nasals, although its extent was variable. It was similarly expressed in all skulls of *Lepus europaeus* consulted by us, as well as in the skulls of *Oryctolagus cuniculus*, *Sylvilagus aquaticus*, and *S. floridanus*, but absent in all studied specimens of *Ochotona* (see

**Supplementary Material**). Thus, this character in *Palaeolagus* shows similarity to leporids (not ochotonids), and the variability in the extent of this character in *P. haydeni* is comparable to the intraspecific variability in *L. europaeus* or *O. cuniculus*.

The ventral surface of the nasal bears a longitudinal nasoturbinates (ethmoidal) crest, which contacts the nasoturbinates and extends posteriorly just anterior to the base of the frontal process. The nasoturbinates crest separates the posterior portion of the ventral surface of the nasal into two concave areas: the medially located dorsal nasal meatus and the laterally located roof of the ethmoidal fossa. The ethmoidal fossa spans above the dorsal surface of the lateral part of the ethmoid labyrinth and is also bordered anteriorly by an anteriorly convex transverse septum, and laterally by the premaxillary process of the nasal. The ethmoidal fossa in *P. haydeni* is relatively shallow dorsoventrally, a condition similar to that in *Ochotona* (*O. dauurica*; ISEZ M/1674/60), but in marked contrast to *Oryctolagus cuniculus*, in which the ethmoidal fossa is greatly expanded dorsoventrally and mediolaterally and forms the 'marsupium nasale' (Krause, 1884).

The premaxillary process of the nasal is a vertically oriented, mediolaterally flattened and slightly laterally convex sheet of bone. Its dorsoventral height is greatest at approximately its anteroposterior mid-length, where the premaxillary process contacts the anterior wall of the ethmoidal fossa and forms

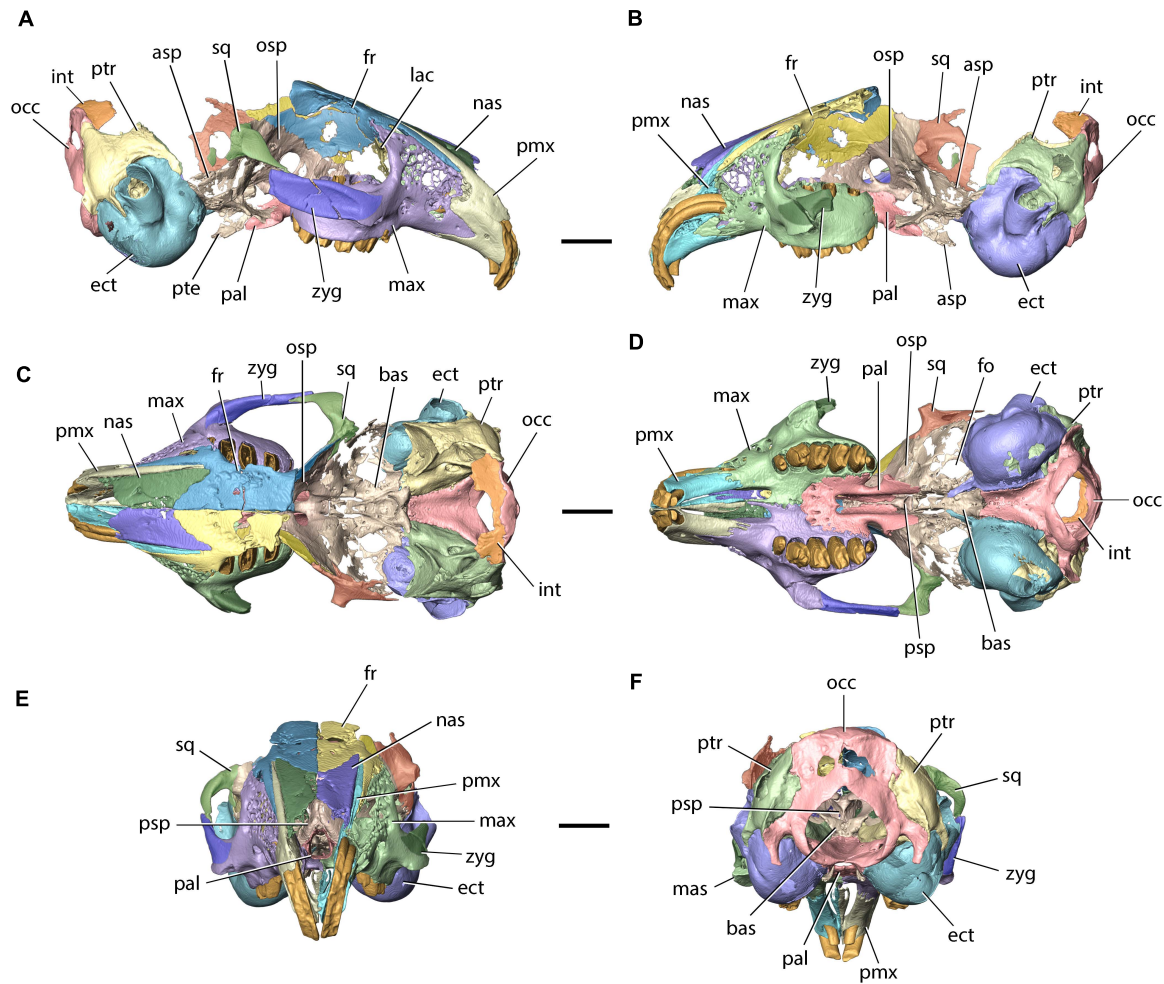


**FIGURE 3** | Model of the cranium of *Palaeolagus haydeni* (FMNH PM9476) in (A) left lateral, (B) right lateral, (C) dorsal, (D) ventral, (E) anterior, and (F) posterior views. asp, alisphenoid; bas, basisphenoid; ect, ectotympanic; fo, foramen ovale; fr, frontal; int, interparietal; lac, lacrimal; mas, masseteric spine; max, maxilla; nas, nasal; occ, occipital; osp, orbitosphenoid; pal, palatine; pmx, premaxilla; psp, presphenoid; pte, pterygoid; ptr, petrosal; sq, squamosal; zyg, zygomatic. Scale bars = 10 mm.

a sharp apex in lateral view. A similar, sharp apex of the premaxillary process is also present in *Ochotona* (*O. dauurica*; ISEZ M/1674/60). Wible (2007, p. 216) also recognized the presence of a sharp apex formed by the nasal in *Ochotona*, but mistook it as part of the nasoturbinates crest. The dorsoventral height of the premaxillary process decreases both anteriorly and posteriorly. The lateral surface of the premaxillary process contacts the medial surface of the nasal process of the premaxilla throughout its entire anteroposterior length.

Posteriorly, the nasal produces a frontal process, which tapers into a sharp apex, posterolaterally, and overlaps a dedicated facet on the anterior portion of the frontal. The posteromedial margins of the frontal processes form a V-shaped suture with the anterolateral margins of the nasal processes of the frontals, a condition similar to that present in leporids, but different from *Ochotona*, in which the frontal processes are rounded posteriorly (Wood, 1940; Wible, 2007, char. 1; Fostowicz-Frelik et al., 2010). The medial margins of both nasals form a straight

internasal suture extending along the dorsal midline of the skull, and a nasoethmoidal suture with the dorsal margin of the nasal septum, ventrally.

### Premaxilla

The paired premaxillae form the anterolateral portions of the rostrum, contribute to the anterior part of the palate and carry both pairs of upper incisors (Figures 3, 4F–J). In FMNH PM9476, the right premaxilla is well preserved, with the exception of its anterior surface, which is slightly abraded, whereas the right premaxilla is extensively damaged, anteriorly. The premaxilla can be divided into a corpus (body) and three processes: a nasal process, a palatine process, and a maxillary process.

The premaxillary corpus bears the alveoli for both pairs of upper incisors. The anterior openings of both alveoli are located anteroventrally. The alveolus for the anterior upper incisor (nominally dI2) is proportionally larger and located more anteriorly and dorsally relative to the alveolus for the

posterior upper incisor (I3). Both alveoli are dorsally curved and extend posteriorly along the entire anteroposterior length of the premaxillary corpus; the dI2 alveolus forms a posterior opening and continues inside the corpus of the maxilla, whereas the I3 alveolus is contained entirely within the body of the premaxilla and extends posteriorly to the base of the maxillary process. The position of both incisors on the lateral surface of the corpus is indicated by the presence of distinct alveolar juga, with the jugum for dI2 being much more prominent. The lateral surface of the premaxillary corpus bears several minuscule neurovascular foramina, dorsally. In some specimens (e.g., USNM PAL 243590 or 2530-49) the dorsal foramina may be extended to a form of substantial fenestration, whereas foramina occurring more ventrally may become more frequent but maintain their minuscule size. The anterodorsal margin of the corpus of the premaxilla, above the incisor alveoli, forms a thin erect lamella confluent with the base of the nasal process. It arises toward the nasals, participating in the formation of the lateral wall of the nasal cavity. Anteriorly, the margin of the lamella is slightly indented (concave) but this 'concavity' does not extend posteriorly beyond the external exposure of dI2. Wood (1940, p. 282) referred to the structure described here as a 'notch' between the nasals and the premaxilla. He also noted that the extent of this concavity and the height of the vertical lamella differentiated *P. haydeni* from extant leporids, which he considered to possess a much more extensive concavity, extending further posteriorly. Furthermore, Wood (1940) stated that this lack of a well-developed 'notch' in *Palaeolagus* resembles the condition found in ochotonids (namely, extant *Ochotona*), and perceived it as a primitive feature. The observations made by Wood (1940) generally hold true; all specimens of *Palaeolagus* studied by us have indeed a very poorly developed 'notch' in which they are similar to *Ochotona* and *Prolagus* (Dawson, 1969). On the other hand, comparisons with a broad sample of extant lagomorphs indicate that this character is much more variable within Leporidae. Most genera have higher and well-developed vertical laminae and the anterior concavity (see Ge et al., 2015), which makes the external nasal aperture higher and the anterior part of the nasal cavity potentially more spacious. The exception is *Romerolagus diazi*, which has the 'notch' very poorly expressed (Wible, 2007) and is similar in this respect to *Ochotona* (Fostowicz-Frelik et al., 2010).

Posterolaterally, the premaxillary corpus forms a triangularly incised suture with the anterior prongs formed by the corpus of the maxilla, with the facet for the dorsal prong exhibiting a small degree of fenestration. The medial surface of the premaxillary corpus contacts the maxilloturbinal, posteriorly, and bears a deep, dorsally curved fossa, which separates the upper incisors and forms the premaxillary portion of the nasolacrimal canal (see **Figure 5E**; Frahnert, 1999; Wible, 2007, char. 11). Anteromedially, the body of the premaxilla forms a mediolaterally compressed vertical plate, which bears a series of anteroposteriorly elongate ridges and troughs. These interlock tightly with ridges and troughs located on the contralateral premaxilla and form the anterior portion of the interpremaxillary suture. As a result, the interpremaxillary suture forms shallow interdigitations in anterior view (**Figure 3E**),

whereas it is straight in palatal view (**Figure 3D**). The anterior margins of the premaxillary corpora form the ventral margin of the external nasal aperture. Their ventromedial margins form the anterolateral margins of the incisive foramina and their posteroventral surfaces contribute to the anterior portions of the diastemata.

The nasal process of the premaxilla [=frontal process of Krause (1884) and Craigie (1948); =posterodorsal process of Wible (2007)] extends posterodorsally from the corpus. It is anteroposteriorly elongate, dorsally curved and sub-triangular in cross-section, forming a sharp, ventral margin. In *P. haydeni*, the nasal process of the premaxilla terminates just anterior to the apex of the frontal process of the nasal, resembling the condition in leporids, but differs from ochotonids, in which the nasal process terminates well anterior to the posterior margin of the nasal (Wood, 1940; Wible, 2007). The medial surface of the nasal process contacts the lateral surface of the premaxillary process of the nasal along its entire anteroposterior length. The ventrolateral surface of the nasal process contacts the maxillary process of the frontal, which separates the premaxilla from the maxilla in dorsal view.

The palatine process of the premaxilla extends posteriorly from the anteromedial surface of the premaxillary corpus. It is anteroposteriorly elongate, mediolaterally narrow and terminates in a blunt apex, posteriorly. It attains its greatest mediolateral width at approximately the anterior three-fourths of its anteroposterior length. In *P. haydeni*, the base of the palatine process of the premaxilla is located at the level of dI2, which differs markedly from the condition in extant leporids and ochotonids, in which the base of the palatine process is located well posterior to I3 (Troxell, 1921; Wood, 1940; Wible, 2007). The palatine process produces a dorsoventrally short, horizontal medial wall and a proportionally taller, laterally convex lateral wall. The dorsal surface of the palatine process is concave and forms a dorsal sulcus [=palatine semisulcus of Krause (1884); =palatine groove of Craigie (1948)], which receives the ventral portion of the cartilaginous internasal septum. Posterolaterally, the palatine process is perforated by an anteroposteriorly elongate foramen, which in extant leporids is filled with a thin layer of connective tissue and does likely not transmit any nerves or vessels (*O. cuniculus*, ZPAL comparative collection). The medial surfaces of both contralateral palatine processes contact each other and form a straight posterior portion of the interpremaxillary suture. The palatine processes separate the anterior portions of both incisive foramina along the ventral cranial midline. The incisive foramen is anteroposteriorly elongate and mediolaterally narrow, anteriorly, but becomes mediolaterally broad posterior to the premaxillary-maxillary suture. It is similar in outline to the incisive foramen in extant leporids, but differs markedly from the bipartite incisive foramen of extant ochotonids (Wible, 2007, char. 32). The incisive foramen is bordered by the premaxilla, anteromedially (palatine process) and anterolaterally (corpus), and by the maxilla (palatine process), posteriorly.

The maxillary process of the premaxilla originates from the posteroventral portion of the premaxillary corpus. It is anteroposteriorly much shorter than the nasal process,

dorsoventrally compressed, and tapers posteriorly into a broad apex. The maxillary process bears several longitudinal ridges, separated by troughs, both dorsally and ventrally. The posterior portion of the maxillary process is entirely encompassed by the anteroventral portion of the maxillary corpus, with the two bones forming an interdigitating premaxillary-maxillary suture in ventral view. The maxillary process of the premaxilla differentiates *P. haydeni* from extant leporids and ochotonids, in which the premaxilla does not form a distinct maxillary process (Wood, 1940; Wible, 2007).

## Frontal

The paired frontals occupy the anterior part of the skull roof and form the posterior roof of the nasal cavity. They also form the dorsal portions of the orbital walls. In FMNH PM9476, both frontals are well preserved anteriorly, but the supraorbital processes, as well as the posterior parts of the frontal squamae, are missing (Figures 3A–C, 4K–L) [compare with Wood, 1940, pl. XXXIV, Figures 2–2a].

The frontal can be divided into a frontal squama and an orbital portion, which are separated from each other by the supraorbital rim (infraorbital margin). The frontal squama forms the anterior part of the skull roof and the posterior portion of the dorsal wall of the nasal cavity. It is dorsoventrally compressed and has an approximately flat dorsal surface, resembling in this respect the frontal of extant ochotonids, but it differs from leporids, in which the part posterior to the supraorbital processes is markedly convex (Wood, 1940; Wible, 2007). This feature is immediately related to the degree of the skull arching, which is much stronger in leporids (Wible, 2007; Fostowicz-Frelik et al., 2010; Fostowicz-Frelik and Meng, 2013) and results in the rounded roof of the braincase in this group. Anteromedially, the frontal squama in *Palaeolagus* forms a nasal process, which is approximately triangular in outline and tapers anteriorly into a broad apex. This differs from the condition present in most leporids, in which the nasal process terminates with a pointed nasal spine (Krause, 1884; Wood, 1940; Craigie, 1948; Wible, 2007), although in some speciose genera (e.g., *Lepus*) the exact morphology of the nasal spine of the frontal may vary from more to less pointed (Koby, 1959). Anterolaterally, the frontal squama forms an anteroposteriorly elongate and laterally curved maxillary process, which is approximately triangular in cross-section and tapers anteriorly into a sharp apex. The maxillary process contacts the nasal process of the premaxilla, medially, and the dorsal margin of the maxillary corpus, ventrolaterally, separating both bones from each other in dorsal view. Posterolaterally, the maxillary process produces an anterolateral prong, which has a rugose posterolateral surface and contacts the dorsomedial surface of the frontal process of the maxilla. The frontal squama also forms a dorsoventrally thin facet for the reception of the frontal process of the nasal, which is much thinner than the remainder of the bone and spans between the lateral margin of the nasal process and the medial margin of the maxillary process. The dorsal surface of the frontal squama is pitted, although not as extensively as in *Romerolagus* or *Sylvilagus* (Wood, 1940; Wible, 2007), and differentiates *Palaeolagus* from extant ochotonids, in which the dorsal surface of the frontal is smooth (Wible, 2007, char. 6).

The pitting of the frontals in *Palaeolagus* clearly delineates the position of the olfactory bulbs (see Figures 4K–L).

In ventral view, the anterior part of the frontal squama forms two concave surfaces (Figure 4L). The medial surface forms the posterior extension of the dorsal nasal meatus, whereas the lateral surface forms an articular surface for the ethmoid. Posteriorly, the ventral surface of the frontal squama forms well-developed fossae for the olfactory bulbs, anteriorly, and the anterior portion of the cerebral fossa, posteriorly (compare with López-Torres et al., 2020). Both fossae are separated from each other by a well-developed transverse ridge, which extends onto the medial wall of the orbital portion of the frontal. The frontal squamae form an approximately straight suture along the dorsal cranial midline.

The orbital portion of the frontal is a medially concave, mediolaterally compressed sheet of bone which forms the dorsal part of the orbital wall. The lateral surface of the orbital portion bears a single ethmoidal foramen, which extends into an ethmoidal sulcus, posteroventrally. Anteriorly, the orbital portion of the frontal abuts against the posterior surface of the frontal process of the maxilla. The orbital portion of the frontal also contacts (from anterior to posterior): the lacrimal, the orbitosphenoid, the squamosal, and the parietal.

## Maxilla

The paired maxillae form the posterolateral portions of the rostrum and the central portion of the palate. They also bear all the cheek teeth, contribute to the anterior orbital margin and comprise the ventral and ventromedial portions of the orbital walls (Figures 3A–E, 5). In FMNH PM9476, both maxillae are well preserved, except for the anterior portion of the left maxillary corpus, which is extensively damaged.

The maxilla can be divided into a corpus (body) and four processes: a frontal process, an alveolar process, a palatine process, and a zygomatic process. The corpus of the maxilla is approximately trihedral in shape and produces two prongs, anteriorly, which insert into dedicated facets on the posterolateral surface of the corpus of the premaxilla. The dorsal prong has a rounded anterior margin (contra Wood, 1940, pl. XXXIV, Figure 2), whereas the ventral prong is anteroposteriorly longer than the dorsal one and tapers anteriorly into a pointed apex. The presence of two anterior maxillary prongs was said to differentiate *P. haydeni* from extant leporids and ochotonids (Wood, 1940), but whereas the maxilla does not bifurcate anteriorly in leporids, it does produce two prongs in some ochotonids, although the ventral prong is not as well developed as in *P. haydeni* (Wible, 2007; Fostowicz-Frelik et al., 2010). The anteroventral portion of the maxillary corpus also bears a dorsoventrally narrow fissure, bordered by a series of anteroposteriorly elongate ridges and troughs, which interlock tightly with a series of corresponding structures located on the dorsal and ventral surfaces of the maxillary process of the premaxilla and produce an interdigitating premaxillary-maxillary suture in ventral view. The posterior portion of the maxillary corpus [=orbital process of maxilla of Craigie (1948)], is thickened and concave, and forms the anterior orbital margin. In addition, it forms the lateral border of the ‘pars orbitalis’ of the maxillary fenestra (Wible, 2007, char. 9).

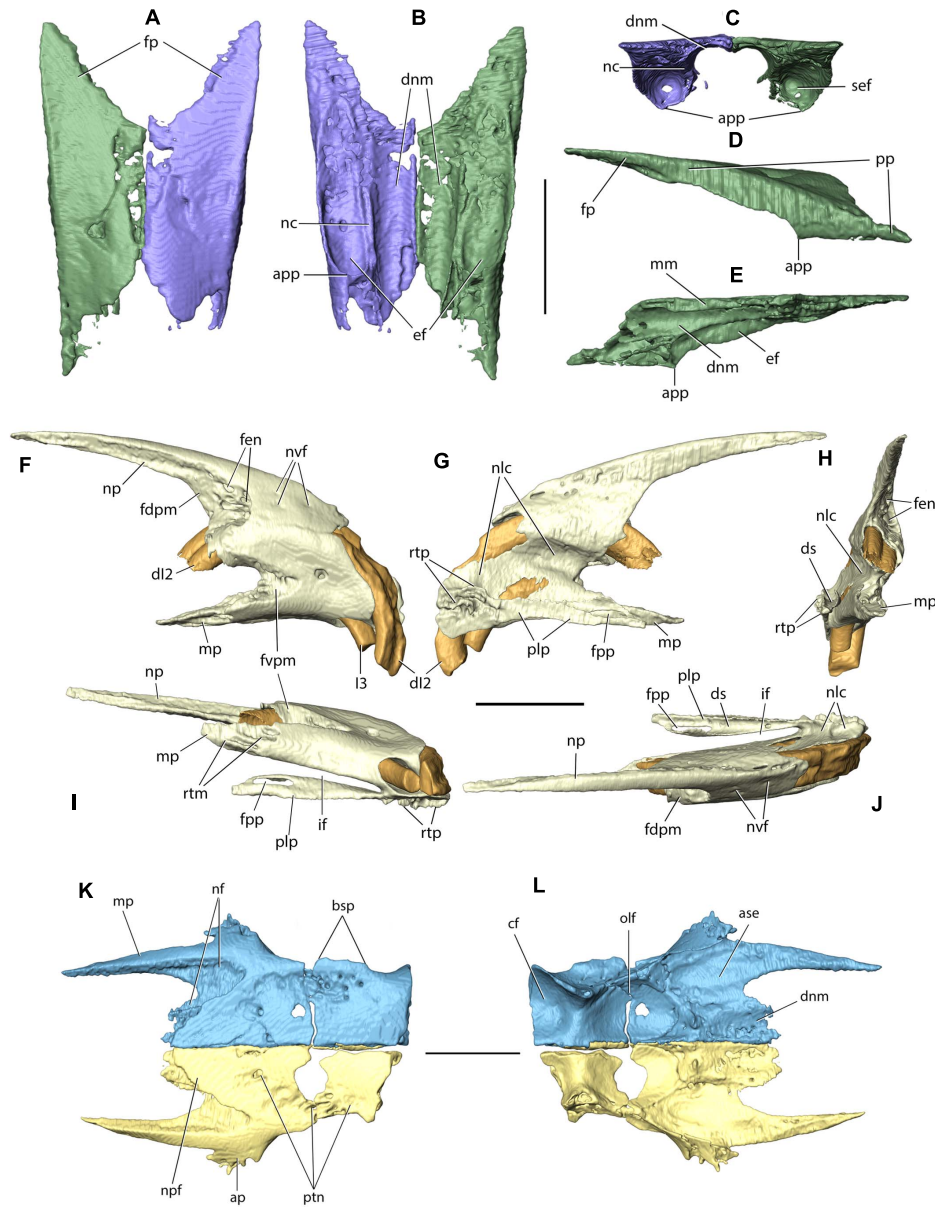


**FIGURE 4 |** Nasal, premaxilla (incisive), and frontal of *Palaeolagus haydeni* (FMNH PM9476). Posterior portions of the left (purple) and right (green) nasals in **(A)** dorsal, **(B)** ventral, and **(C)** posterior views. Right nasal in **(D)** lateral and **(E)** medial views. Right premaxilla in **(F)** lateral, **(G)** medial, **(H)** posterior, **(I)** ventral, and **(J)** dorsal views. Left (yellow) and right (blue) frontals in **(K)** dorsal and **(L)** ventral views (orbital portions removed). ap, anterior prong; app, apex of premaxillary process; ase, articular surface for ethmoid; bsp, base of supraorbital process (broken); cf, cerebral fossa; dnm, dorsal nasal meatus; ds, dorsal sulcus; ef, ethmoidal fossa; fdpm, facet for dorsal prong of maxilla; fen, fenestration; fp, frontal process; fpp, foramen in palatine process; fvpm, facet for ventral prong of maxilla; dl2, anterior upper incisor; l3, posterior upper incisor; if, incisive foramen; mm, medial margin; mp, maxillary process; nc, nasoturbinate (ethmoidal) crest; nf, nasal facet; nlc, nasolacrimal canal; np, nasal process of premaxilla; npf, nasal process of frontal; nvf, neurovascular foramen; olf, olfactory bulb fossa; plp, palatine process; pp, premaxillary process; ptn, pitting; rtm, ridges and troughs for maxilla; rtp, ridges and troughs for contralateral premaxilla; sef, anterior septum of ethmoidal fossa. Scale bars = 5 mm.

The lateral wall of the maxillary corpus is perforated by a lacework of small openings, similar to that present in extant leporids, but different from ochotonids, in which the lateral wall of the maxillary corpus produces a large, single opening ('pars facialis' of the maxillary fenestra; Wible, 2007, char. 8). Posteroventrally, the lateral surface of the maxillary corpus

bears a large, sub-circular infraorbital foramen for the passage of the infraorbital nerve (branch of the maxillary nerve [CN V<sub>2</sub>]) and associated blood vessels. Anteriorly, the infraorbital foramen opens into the maxillary fossa located on the external surface of the bone, whereas posterodorsally it extends into the infraorbital canal located on the medial surface of the lateral wall

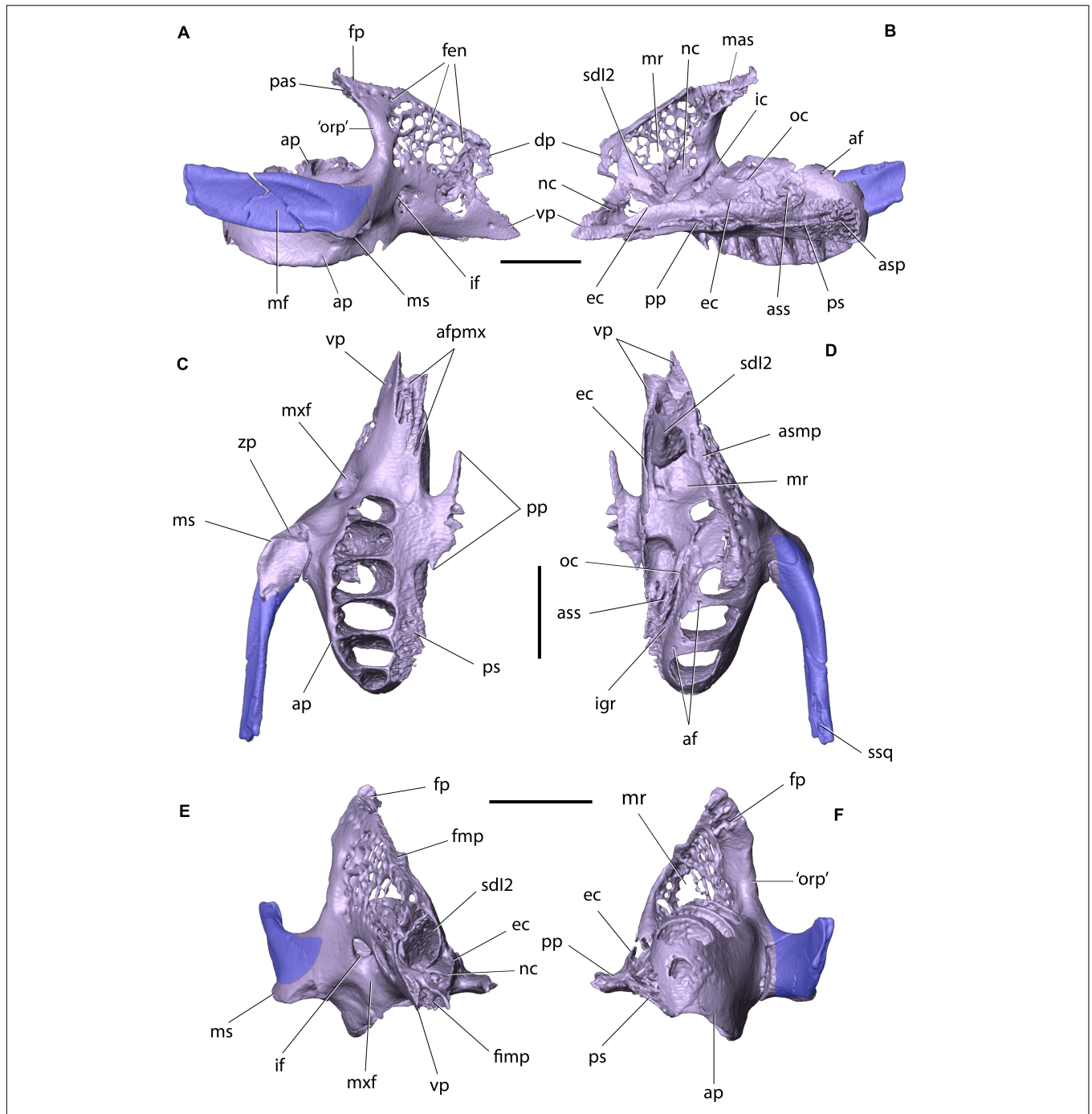


**FIGURE 5 |** Right maxilla and zygomatic of *Palaeolagus haydeni* (FMNH PM9476) in: **(A)** lateral, **(B)** medial, **(C)** ventral, **(D)** dorsal, **(E)** anterior, and **(F)** posterior views. Dentition removed for clarity. af, alveolar foramen; afpmx, articular facet for maxillary process of premaxilla; ap, alveolar process; asp, articular surface for horizontal lamina of palatine; ass, articular surface for ethmoidal process of presphenoid; dp, dorsal prong; ec, ethmoidal crest; fen, fenestrations; fimp, fissure for maxillary process of premaxilla; fmp, facet for maxillary process of frontal; fp, frontal process; ic, infraorbital canal; if, infraorbital foramen; igr, infraorbital groove; mas, dorsomedial articular surface of frontal process; mf, masseteric fossa; mr, maxillary recess (sinus); ms, masseteric spine; mx, maxillary fossa; nc, nasolacrimal canal; oc, orbital crest; 'orp', 'orbital process' (posterior part of the corpus); pas, posterior articular surface of frontal process; pp, palatine process; ps, palatine shelf; sd12, sheath for d12; ssq, sulcus for zygomatic process of squamosal; vp, ventral prong; zp, zygomatic process. Scale bars = 5 mm.

of the premaxillary corpus. Anterodorsal to the infraorbital canal, the medial surface of the lateral wall of the maxillary corpus forms the maxillary portion of the nasolacrimal canal, which

extends anteroventrally from the level of the 'pars orbitalis' of the maxillary fenestra, and attains a sub-sagittal orientation at the level of the posterior end of d12, as in extant leporids (**Figure 6E**;

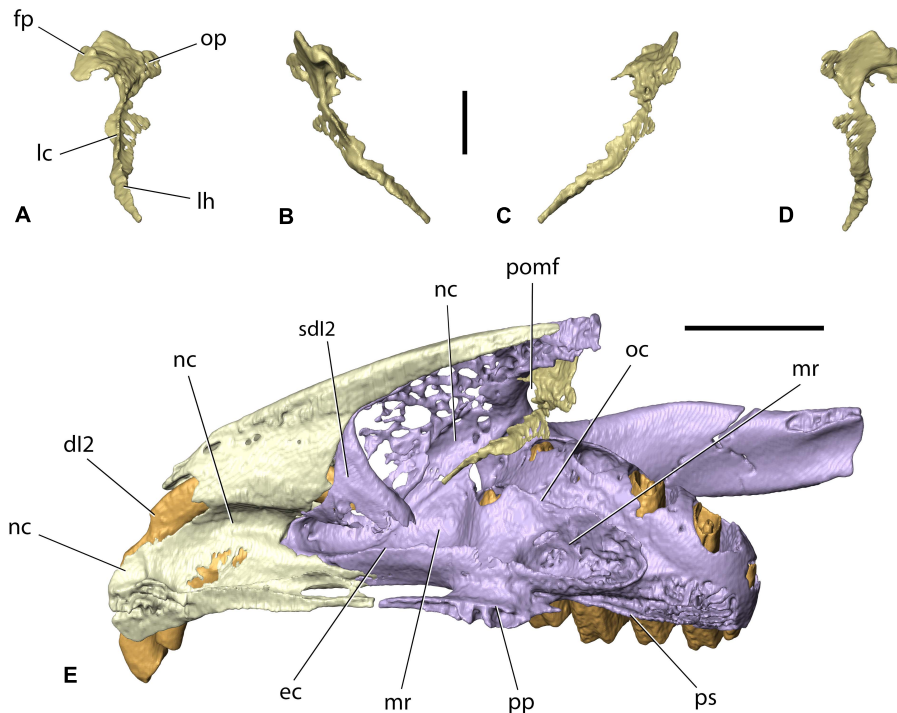


**FIGURE 6** | Right lacrimal of *Palaeolagus haydeni* (FMNH PM9476) in (A) anterior, (B) lateral, (C) medial, and (D) posterior views. Note the incompleteness of the facial process and orbital plate. (E) Right premaxilla (light yellow), lacrimal (gold) and maxilla-zygomatic complex (light purple) in dorsomedial view, highlighting the position of the nasolacrimal canal. Teeth marked with orange. fp, facial process; dl2, anterior upper incisor; lc, lacrimal crest; lh, lacrimal hamulus; mr, maxillary recess (sinus); nc, nasolacrimal canal; oc, orbital crest; op, orbital plate; pomf, 'pars orbitalis' of maxillary fenestra; pp, palatine process; ps, palatine shelf; sdl2, sheath for dl2. Scale bar in (A–D) = 2 mm; scale bar in (E) = 5 mm.

Frahnert, 1999; Wible, 2007, char. 11). Dorsally, the maxillary corpus bears a longitudinal facet for the reception of the maxillary process of the frontal. The posterior surface of the maxillary corpus abuts against the facial process of the lacrimal, dorsally. The ventral surface of the maxillary corpus forms the posterior portion of the diastema, and its ventromedial margin forms the posterolateral margin of the incisive foramen.

Anteromedially, the maxillary corpus forms a sheath for the posterior portion of dl2. Ventromedially, it bears a longitudinal, dorsoventrally low ethmoidal crest, which contacts the ethmoid, anterolaterally and dorsally, and the palatine, posteromedially. Adjacent to the alveolar process, the body of the maxilla forms an orbital crest, which contacts the orbitosphenoid, medially. The external exposure of the crest is anteroposteriorly much more elongate than that visible in lagomorphs and ochotonids (Wible, 2007, char. 14), but is similar to the anteroposteriorly elongate orbital crest (=process) visible in the medial orbital wall in *Rhombomylus turpanensis* (Meng et al., 2003, Figure 31). Several recesses are present within the maxillary corpus, which collectively form the maxillary recess (sinus). Posterodorsally, the maxillary corpus produces a frontal process (=sphenoorbital process of Craigie, 1948). The dorsomedial and posterior surfaces of the frontal process are rugose and abut against corresponding surfaces on the anterior prong of the maxillary process of the frontal, and the orbital portion of the frontal, respectively. The lateral

wall of the frontal process is fenestrated and perforated by several small foramina.

The alveolar process carries the cheek teeth and is located posterolateral to the maxillary corpus. The alveolar process in *P. haydeni* represents a morphology somewhat intermediate between that in extant leporids and ochotonids, in that it is not as mediolaterally broad as in ochotonids, in which the process forms the ventral portion of the orbital wall, but it is also not as medially shifted as in leporids. The alveolar process is also relatively lower than in extant leporids, which is related to proportionally lower tooth crowns in *Palaeolagus*.

Posteriorly, the alveolar process in *P. haydeni* remains relatively broad mediolaterally and possesses a convex, posterior surface, resembling the alveolar process of *Ochotona*. In contrast, in extant leporids the mediolateral width of the alveolar process decreases posteriorly (Wood, 1940; Wible, 2007; Fostowicz-Freluk and Meng, 2013). The alveolar process bears six alveoli (P2–4 and M1–3). The alveolus for M1 is the largest and the size of the remaining alveoli decreases both anteriorly and posteriorly, with the M3 alveolus being the smallest. Several small alveolar foramina are present on the dorsal surface of the alveolar process. Medially, the alveolar process is separated from the orbital crest by a deep, oblique infraorbital groove for the infraorbital nerve and vessels (Fostowicz-Freluk and Meng, 2013). The infraorbital groove in *P. haydeni* resembles the deep groove present in leporids but differs markedly from the shallow groove present in

ochotonids (Fostowicz-Frelik and Meng, 2013). This character is related to the degree of mediolateral displacement of the alveolar process (see above). The infraorbital groove ends anteriorly at the infraorbital foramen, through which the infraorbital nerve and vessels pass onto the external surface of the maxilla (Fostowicz-Frelik and Meng, 2013). The pulp cavities of the cheek teeth are exposed on the dorsal surface of the alveolar process in FMNH PM9476, a feature which has been demonstrated to vary within *P. haydeni* (Wood, 1940) and is also present in most leporids, but has not been observed in ochotonids (Wible, 2007, char. 16). Posterioventromedially, the alveolar process forms a complex palatomaxillary suture with the perpendicular portion of the palatine, comprising of: (1) an anteroposteriorly elongate, slightly medially inclined palatine shelf, which inserts into a deep groove located in the lateral surface of the palatine, and (2) a series of anteroposteriorly elongate projections, which interlock tightly with corresponding projections located on the lateral surface of the perpendicular portion of the palatine.

The palatine process extends laterally from the ventral portion of the maxillary corpus and forms the anterior portion of the hard palate (palatine bridge). The palatine process is dorsoventrally flattened and produces a mediolaterally narrow spine, anteromedially, which ends with a blunt apex that almost contacts the apex of the palatine process of the premaxilla. As a result, the left and right incisive foramina are almost completely separated from each other along the ventral midline of the skull in *P. haydeni*, a condition similar to that present in leporids, but markedly different from the condition present in ochotonids, in which the palatine processes of the premaxilla and maxilla are well separated from each other (Wible, 2007, char. 32; Ge et al., 2015). Posterodorsally, the palatine process is overlapped by the horizontal portion of the palatine. Medially, each palatine process produces a series of prominent prongs which interlock tightly with the prongs present on the contralateral palatine process and form the intermaxillary suture. The lateral and posterior margins of the palatine process form the medial and posterior margins of the incisive foramen, respectively.

The zygomatic process of the maxilla extends laterally from the maxillary body, at the level of P2–P3. Anteroventrolaterally, it forms a well-developed masseteric spine, which served as the attachment for the ligament of the masseteric muscle, as in *O. cuniculus* (Craigie, 1948). Like in osteologically mature specimens of extant lagomorphs, the zygomatic process of *P. haydeni* is tightly co-ossified with the anterior portion of the zygomatic, so that the suture between both elements is usually not discernible (Craigie, 1948; Wible, 2007).

## Lacrimal

The lacrimal lies appressed against the anterior wall of the orbit. It comprises an anteroposteriorly compressed orbital plate, a facial (lateral) process, and the lacrimal hamulus. In FMNH PM9476, only the right lacrimal is partially preserved (Figures 3B, 6A–D). Its orbital plate and facial process are abraded to a large extent, whereas the lacrimal hamulus is well preserved. Wood (1940, p. 281) noted that the orbital plate of the lacrimal in *P. haydeni* was extensive, like in extant lagomorphs, and occupied much of the anteromedial orbital wall. However, the lacrimal in *P. haydeni*

was not figured either by him or by earlier authors (see Troxell, 1921; Dice, 1933). Even though the orbital plate is not preserved in the right lacrimal in FMNH PM9476, its presence can be inferred from the presence of large openings in the anteromedial walls of both orbits, which resemble the openings visible in extant leporid specimens with disarticulated lacrimals (Wood, 1940; Wible, 2007). The lacrimal hamulus extends anteroventrally from the orbital plate and tapers into a pointed apex. Laterally, the hamulus forms the medial wall of the posterior portion of the nasolacrimal canal (Figure 6E). Dorsally, the hamulus produces a lacrimal crest, which extends along its entire anteroposterior length. The concave, lateral margin of the lacrimal forms the medial margin of the orbital portion ('pars orbitalis') of the maxillary fenestra (Wible, 2007). The orbital portion of the maxillary fenestra is a dorsoventrally tall and mediolaterally narrow opening, which is bordered medially by the posterior part of the maxillary corpus forming the anterior orbital rim. Ventrally, the orbital portion of the maxillary fenestra becomes confluent with the infraorbital and nasolacrimal canals.

## Zygomatic (=Jugal)

The zygomatic comprises the anterior portion of the zygomatic arch and forms approximately the anterior two-thirds of the ventral margin of the orbit (Figures 3A–D, 5). In FMNH PM9476, only a small portion of the left zygomatic, adjacent to the zygomatic process of the maxilla, is preserved. In contrast, the right zygomatic is almost completely preserved, with the exception of its posterior portion.

Anteriorly, the zygomatic is extensively fused with the zygomatic process of the maxilla, like in osteologically mature specimens of extant lagomorphs (Craigie, 1948; Wible, 2007). The zygomatic is mediolaterally and dorsoventrally broadest anteriorly. Its dorsoventral height gradually decreases posteriorly, whereas its mediolateral width decreases abruptly posterior to its anterior end and remains constant throughout the remainder of its anteroposterior length. Its dorsal margin is slightly thicker mediolaterally than its ventral margin, which forms a sharp crest. Both the lateral and medial surfaces of the zygomatic are concave, with the concavity on the lateral surface forming a prominent zygomatic fossa, which acted as an attachment site for the lateral masseter muscle. In contrast to extant leporids and ochotonids, the lateral surface of the zygomatic does not bear any neurovascular foramina (Krause, 1884; Wible, 2007, char. 20). The posterodorsal margin of the zygomatic bears a sulcus for the reception of the zygomatic process of the squamosal. The posterior portions of the zygomatic bones are not preserved in FMNH PM9476, but in more complete specimens of *P. haydeni* (Dice, 1933; Wood, 1940), the zygomatic forms a short, posterior process, similar to that present in the majority of extant leporids, but unlike the elongate posterior process in *R. diazi* and ochotonids (Wible, 2007, char. 21).

## Palatine

The palatine comprises a single, unpaired element, located posterior to the maxillae along the ventral cranial midline (Figures 3D, 7). The unpaired palatine arises as a result of the anterior fusion of paired, embryonic ossifications

(Insom et al., 1990). It forms the posterior portion of the hard palate (palatal bridge), the anteromedial walls of the pterygopalatine fossae and the lateral walls of the nasopharyngeal duct. In FMNH PM9476, the palatine is completely preserved, enabling a detailed description of its anatomy. Each hemipalatine is divided into a medial horizontal lamina (portion) and a lateral perpendicular lamina. The horizontal lamina forms approximately the posterior two-thirds of each half of the hard palate. It has a palatine (ventral) surface, a nasal (dorsal) surface, a convex anterior margin, and a concave posterior margin. The anterior margin, located at the level of the interalveolar septum separating P3 and P4, bears a groove that receives the posterior margin of the palatine process of the maxilla. The posterior margin bears a prominent nasal spine, medially. Anterolaterally, the palatine surface bears a large, sub-circular major palatine foramen. Posteromedially and posteriorly to the major palatine foramen, the palatine surface has two (right) and three (left) additional foramina – the accessory palatine foramina. The posteromedial accessory palatine foramina are small and are preceded anteriorly by anteroposteriorly elongated grooves, whereas the posterior accessory palatine foramina are larger and sub-circular in outline. The presence of a single major palatine foramen, enclosed entirely within the palatine in *P. haydeni*, resembles the condition present in numerous extant leporids, with the exception of *Pronolagus* and *Lepus*, in which the major palatine foramen is bordered anteriorly by the maxilla. In ochotonids, a single major palatine foramen cannot be recognized, but multiple small foramina occupy the anterolateral palatine surface, instead (Wible, 2007, char. 33). All palatine foramina form the ventral openings of palatine canals which perforate the horizontal lamina and open into the sphenopalatine canal.

The perpendicular lamina of the palatine extends dorsally from the lateral border of the horizontal lamina at an approximately right angle. The dorsal margins of both perpendicular laminae converge posteromedially, so that each perpendicular lamina forms a slightly concave lateral wall of the nasopharyngeal canal, medially, and an oblique wall of the pterygopalatine fossa, laterally. The dorsal margin of each perpendicular lamina bifurcates into a medial and lateral crest, which border a deep groove for the reception of the ethmoidal process of the presphenoid, anteriorly, and the presphenoid corpus, posteriorly. The posterodorsal margin of the perpendicular plate is concave and forms the anteromedial boundary of the superior orbital fissure. Anterolaterally, the perpendicular lamina forms an oblique crest, which abuts against the medial wall of the ethmoidal crest of the maxilla, laterally. Ventrolaterally, the perpendicular lamina forms a series of medially projecting shelves, grooves and protrusions, which tightly interlock with corresponding structures present on the medial surface of the alveolar process of the maxilla to form the palatamaxillary suture. Dorsolaterally, the perpendicular plate bears an oblique sphenopalatine canal, which connects the pterygopalatine fossa with the nasal cavity. The canal is bordered by the perpendicular lamina of the palatine, ventrally and medially, by the alveolar process of the maxilla, laterally, and by the ethmoidal process of the presphenoid, dorsally. Anteriorly,

the sphenopalatine canal opens with the sphenopalatine foramen, which is bordered by the alveolar process of the maxilla, laterally, and the horizontal lamina of the palatine, medially, like in extant lagomorphs (Wible, 2007, char. 13; contra Asher et al., 2005, char. 133). Ventrally, the sphenopalatine canal is perforated by minute openings of palatine canals, which lead to the nasal surface of the horizontal lamina and open externally as accessory palatine foramina. Anteriorly, the sphenopalatine canal bifurcates into a large, anteroventral canal, which opens externally as the major palatine foramen, and an anteromedial groove, which leads into the dorsal opening of a canal which opens ventrally as one of the accessory palatine foramina. Posteroventrally, the perpendicular lamina produces a pyramidal (sphenoidal) process, which is separated from the main portion of the lamina by a concave surface. In dorsal or ventral view, this surface forms the palatine notch (incisure) (=posterior maxillary notch of Wahlert, 1974) that transmits the minor palatine nerve and associated vessels. The deep, concave palatine notch in *P. haydeni* resembles the condition present in extant ochotonids, but differs markedly from extant leporids, in which the palatine notch forms a pointed apex (Wible, 2007). The posterior margin of the pyramidal process contacts the medial lamina of the pterygoid and forms the anterior portion of the entopterygoid crest. Posterolaterally, the pyramidal process bears a deep fissure, which receives the anterior portion of the lateral lamina of the pterygoid. The posterior part of the dorsolateral surface of the pyramidal process contributes to the anteromedial wall of the pterygoid fossa.

## Presphenoid

The presphenoid is an unpaired element, which occupies the anterior portion of the cranial floor and contributes to the ventral portions of the orbital walls (Figures 3A,B, 8). In FMNH PM9476, the presphenoid is almost complete, except for the dorsal portion of the right ethmoidal process, which is not preserved. The presphenoid comprises a median corpus (body) and paired ethmoidal processes. The corpus of the presphenoid, which has the form of an anteroposteriorly elongate cylinder, is located along the ventral midline of the skull, anterior to the basisphenoid and posterior to the ethmoid. Posteroventrally, the presphenoid corpus forms a concave facet, which is approximately hexagonal in outline, and forms the anterior boundary of the intersphenoidal synchondrosis. Ventrally, the presphenoid corpus bears a median ridge, bordered laterally by articular surfaces for the perpendicular portions of the palatine. Anterolaterally, the presphenoid forms paired ethmoidal processes. Each ethmoidal process comprises a dorsoventrally tall lateral wall and a concave ventral wall. The lateral wall abuts against the orbital crest of the maxilla, anterolaterally. The ventral wall forms a sharp, ventral crest, which inserts into an anteroposteriorly elongate groove located on the perpendicular lamina of the palatine. The anteroventral corner of the ethmoidal process is encompassed by the maxillary corpus. The anteriorly open space bordered laterally and ventrally by both ethmoidal processes comprises the sphenoidal fossa (sinus). Posterior to the ethmoidal processes, the presphenoid forms the sphenoidal yoke (jugum sphenoidale), which forms the ventral surface of the anterior cranial fossa. Posteroventral to

the optic canal, the presphenoid forms the sulcus chiasmatis for the optic chiasma.

## Orbitosphenoid

The orbitosphenoids (lesser wings) extend posterodorsally from the presphenoid corpus. Posterior to the sphenoidal yoke, the medial margins of the orbitosphenoids bear notches which form the lateral margins of a single optic canal. Posteroventrally to the optic canal, the internal (medial) surfaces of the orbitosphenoids form the sulcus chiasmatis for the optic chiasma. The external (lateral) surfaces of the orbitosphenoids contribute to the posterior portions of the orbital walls, whereas their internal (medial) surfaces form a considerable portion of the anterolateral surface of the middle cranial fossa (Figures 3A,B, 8). The orbitosphenoid also forms the posteromedial boundary of the superior orbital fissure. The orbitosphenoid contacts the orbital portions of the frontal, anterodorsally, the alisphenoid, posteriorly, and fuses with the squamosal, posterolaterally.

## Basisphenoid

The basisphenoid, the alisphenoids and the pterygoids are well preserved in FMNH PM9476, because of limited preparation performed on the external surfaces of the basis cranii (Figure 1D). This is in stark contrast to most other cranial specimens of *P. haydeni*, in which the basisphenoid, alisphenoids and pterygoids are damaged or not preserved (Wood, 1940, p. 285).

The basisphenoid occupies the base of the middle cranial fossa and is located anterior to the basioccipital and posterior to the presphenoid. Its dorsal surface forms a central hypophyseal fossa, bordered posteriorly by the dorsum sellae, which is elevated considerably beyond the dorsal surface of the middle cranial fossa. Anterolaterally, the dorsum sellae produces a pair of prominent posterior clinoid processes, which, together with the hypophyseal fossa and the dorsum sellae, comprise the sella turcica. Lateral to the hypophyseal fossa, the basisphenoid bears a pair of carotid sulci, which mark the passage of the internal carotid arteries, entering the middle cranial fossa though the carotid canal enclosed between the petrosal and ectotympanic bones. The anterior portion of the basisphenoid is mediolaterally narrow and anteroposteriorly elongate and is bordered laterally by sphenopalatine vacuities, which become confluent with the superior orbital fissures, anteriorly. The sphenopalatine vacuity transmits the nerve of the pterygoid canal, which occupies a weakly demarcated groove located posterior to the sphenopalatine vacuity on the ventral surface of the basisphenoid (visible on the left side of FMNH PM9476). *P. haydeni* shares the presence of anteroposteriorly elongate, medially positioned sphenopalatine vacuities with ochotonids and the leporid *Pronolagus*, but differs in this respect from the majority of leporids, in which the sphenopalatine vacuity is smaller and more laterally positioned or is entirely absent (Wible, 2007, char. 36). The ventral surface of the basisphenoid bears a small midline foramen (=foramen cavernosum of Krause, 1884) for the craniopharyngeal canal, which is also present in extant leporids, but absent in ochotonids and *Rhombomylus turpanensis* (Wible, 2007, char. 43). The foramen cavernosum

opens internally into the extensive sphenoidal sinus, clearly visible in FMNH PM9476 because of extensive damage to the anterodorsal surfaces of the basisphenoid. Posterolateral to the posterior margin of the medial lamina of the pterygoid, the basisphenoid is perforated by two (right side) and one (left side) transverse canal foramina, which are also present in both leporids and ochotonids (Wible, 2007, char. 42). Anteriorly, the basisphenoid forms a sub-oval, concave surface, which forms the posterior limit of the intersphenoidal synchondrosis. Posteriorly, it forms a pair of ventrally projecting tuberosities, the posterior surfaces of which abut against the anterior surface of the basioccipital. Posterolaterally, the basisphenoid is underlapped by the styloform processes of the ectotympanic bones.

## Alisphenoid

The alisphenoids (greater wings) extend laterally from the basisphenoid and form the ventrolateral walls of the middle cranial fossa and continue anterodorsally to form the posterior wall of the orbit (Figures 3A,B, 8, 9). Ventromedially to the base of the zygomatic process of the squamosal, the alisphenoid produces a low, sub-transverse ridge, which forms the alisphenoid crest [=crista alae magnae of Craigie (1948)]. In extant lagomorphs, the alisphenoid surface located immediately medial and ventral to the crest is formed by very thin, semi-transparent sheets of connective tissue (*O. cuniculus*, ZPAL comparative collection). Therefore, the large, irregular openings located ventromedially and posterolaterally to the alisphenoid crest in FMNH PM9476 are interpreted as similar areas covered in life by thin connective tissue rather than as any neurovascular openings (Figures 8, 9).

The alisphenoid is perforated by several foramina that connect the middle cranial fossa with the external surface of the cranium and serve as the passageways of important nerves and vessels. The largest opening, located immediately lateral to the basisphenoid, is the sub-oval foramen ovale, which serves as the passageway for the mandibular nerve (CN V<sub>3</sub>). Posterior to the foramen ovale, the dorsal surface of the alisphenoid bears a mediolaterally broad and anteroposteriorly short groove, which indicates the position of the root of the mandibular nerve and the associated semilunar ganglion (Craigie, 1948). The foramen ovale in *P. haydeni* is located entirely within the alisphenoid, whereas in leporids it is bordered posteriorly by the petrosal, as a result of the foramen ovale being confluent with the piriform fenestra; the condition in ochotonids is variable (Wible, 2007, char. 40). FMNH PM9476 does not possess a piriform fenestra posterior to the foramen ovale, but it is possible that some of the spaces preserved lateral to the foramen ovale represent fenestrations homologous to the piriform fenestra present in some lagomorphs (e.g., *Lepus*, ZPAL comparative collection).

The anteromedial margin of the alisphenoid is concave and forms the lateral margin of the superior orbital fissure, which represents both the superior orbital fissure and foramen rotundum present in other mammals and serves as the passage way for CN III, IV, V<sub>1</sub>, V<sub>2</sub> and VI (Craigie, 1948) (Figures 8, 9). The superior orbital fissure does not possess a dedicated medial wall and is bordered medially by the basisphenoid and anteriorly by the posterior margin of the perpendicular lamina

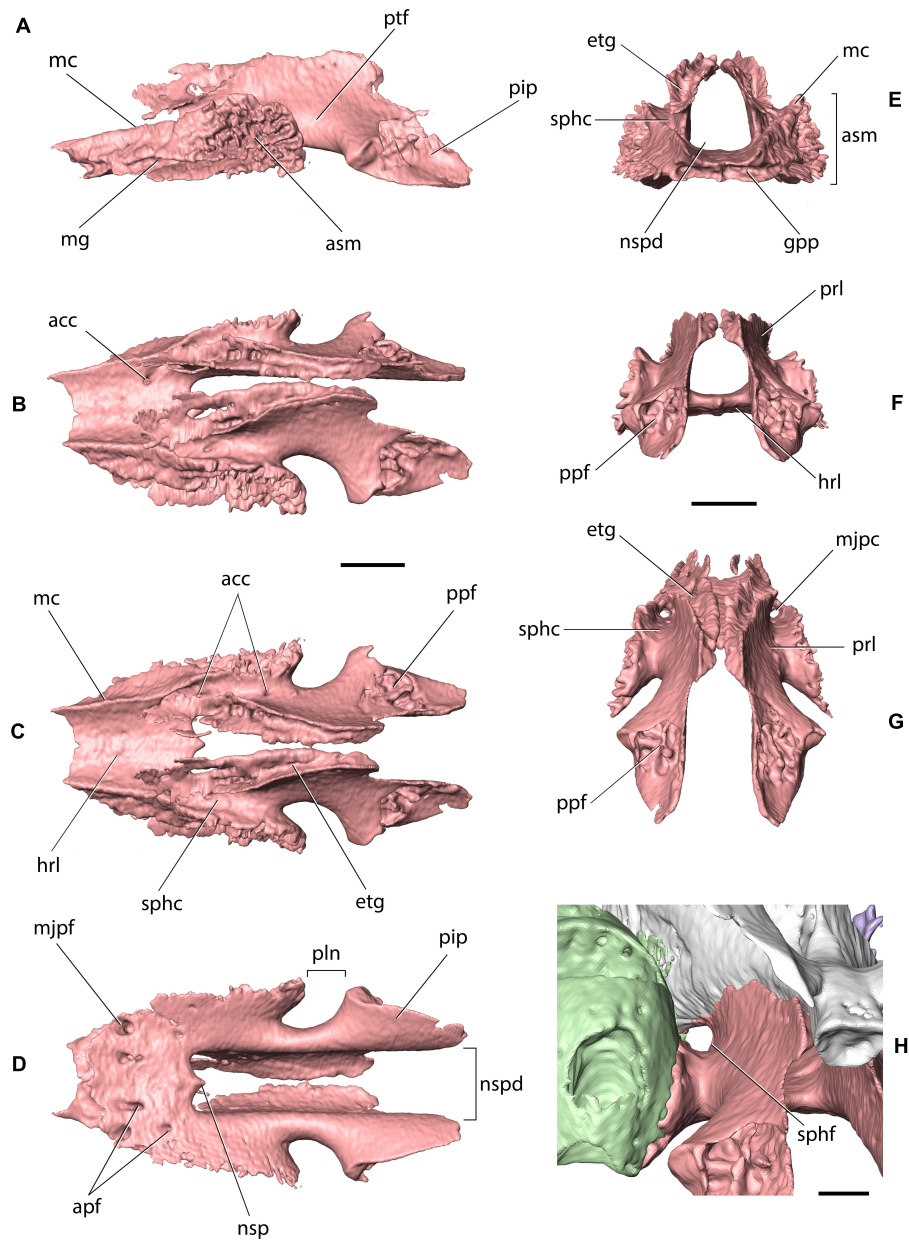


**FIGURE 7 |** Palatine of *Palaeolagus haydeni* (FMNH PM9476) in (A) left lateral, (B) left dorsolateral, (C) dorsal, (D) ventral, (E) anterior, (F) posterior, (G) posterodorsal, and (H) left posterolateral views. Left maxilla shown in light green, presphenoid shown in white. acc, dorsal opening of accessory palatine canal; apf, accessory palatine foramen; asm, articular surface for alveolar process of maxilla; etg, ethmoidal groove; gpp, groove for palatine process of maxilla; hrl, horizontal lamina; mc, maxillary crest; mg, maxillary groove; mjpc, major palatine canal; mjpf, major palatine foramen; nsp, nasal spine; nspd, nasopharyngeal duct; pip, pyramidal process; pln, palatine notch; ppf, fissure for pterygoid process of basisphenoid; prl, perpendicular lamina; ptf, pterygopalatine fossa; sphc, sphenopalatine canal; sphf, sphenopalatine foramen. Scale bars for (A–G) = 2 mm, scale bar for (E) = 1 mm.

of the palatine. Posterolateral to the superior orbital fissure, the base of the lateral lamina of the pterygoid is perforated by the alisphenoid canal, which forms the passage for the maxillary artery and vein (Wible, 2007, char. 38). Lateral to the alisphenoid canal, the base of the lateral lamina of the pterygoid bears a sub-circular foramen, which likely represents the masseteric foramen for the masseterico-temporal ramus of the mandibular nerve, also present in extant lagomorphs (Wible, 2007, char. 39). The

presence of the buccinator foramen cannot be confirmed in FMNH PM9476, due to the incompletely preserved surface of the alisphenoid in the adjacent region.

## Pterygoid

The paired pterygoids, which comprise medial and lateral laminae, extend anterolaterally to the basisphenoid. The medial lamina [=entopterygoid crest of Wible (2007)] is vertical

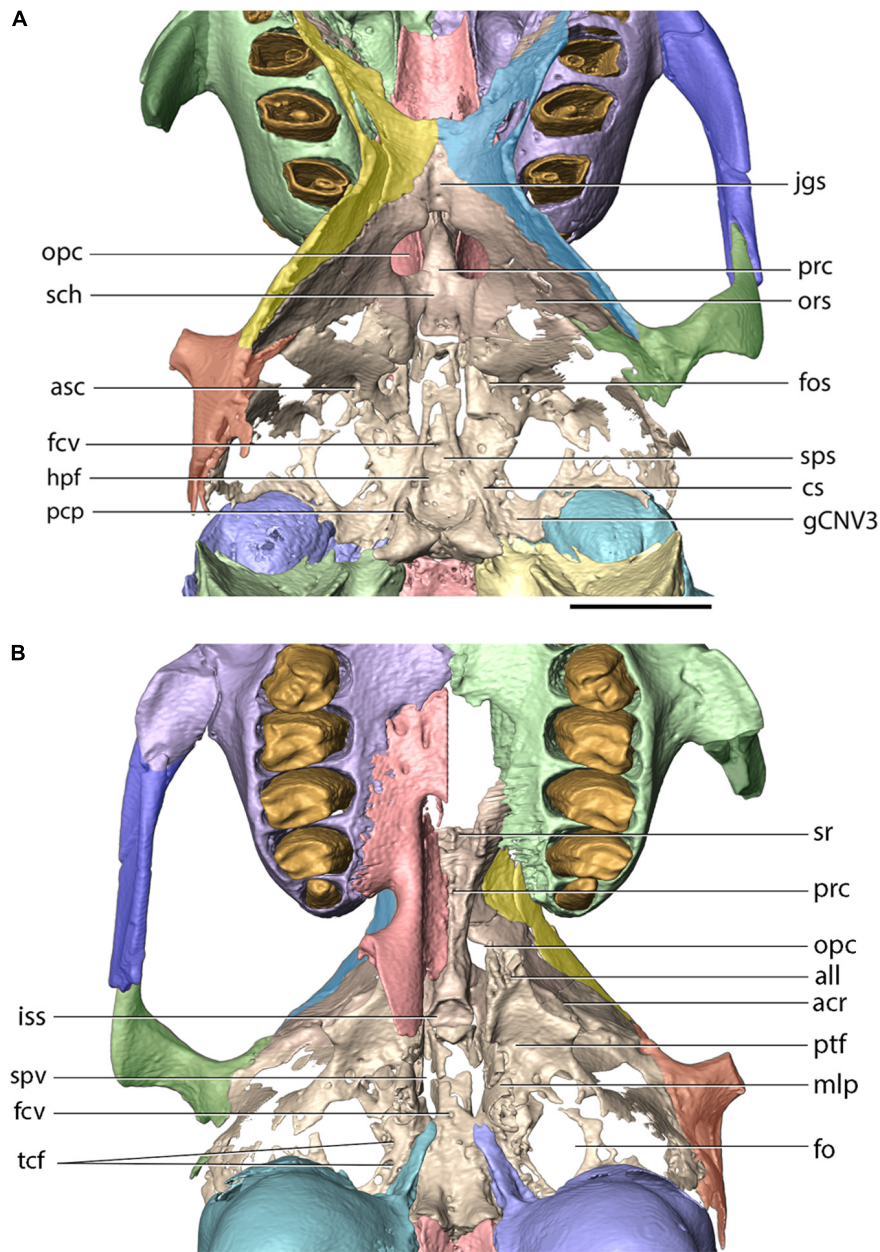
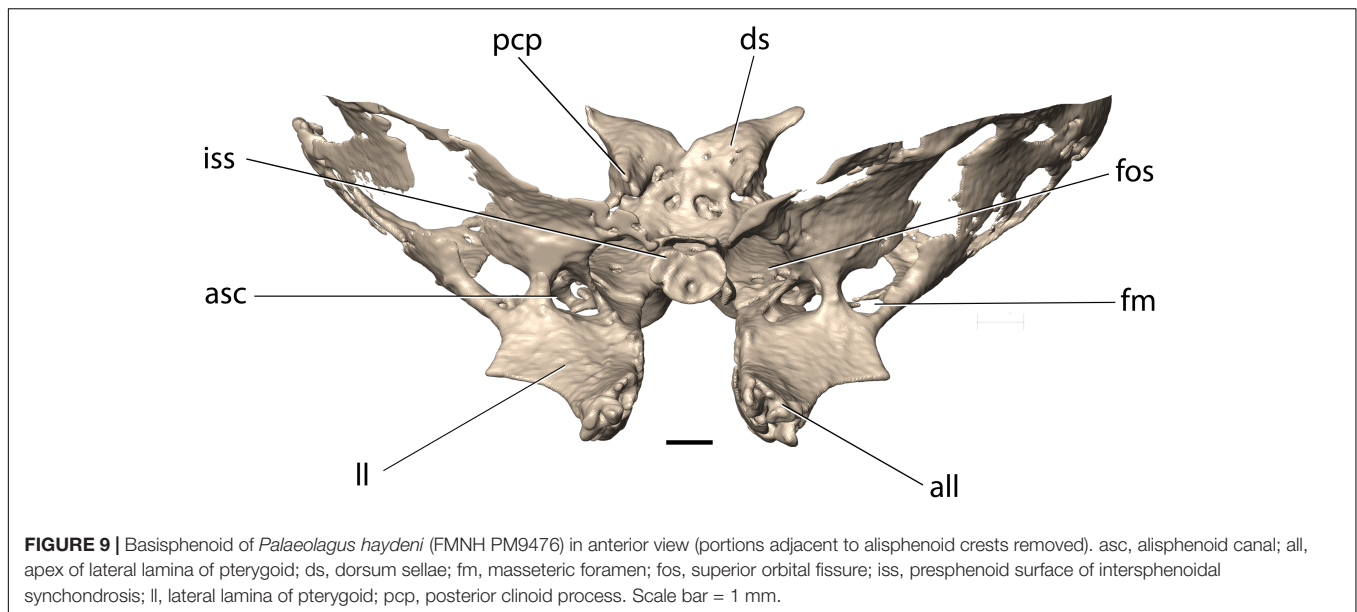


**FIGURE 8** | Cranial base of *Palaeolagus haydeni* (FMNH PM9476) in (A) dorsal and (B) ventral views. Frontal (orbital portion)-presphenoid-basisphenoid-squamosal figured as complex (internal sutures not visible in CT data). acr, alisphenoid crest; all, apex of lateral lamina of pterygoid process; asc, alisphenoid canal; cs, carotid sulcus; fcv, foramen cavernosum; fo, foramen ovale; fos, superior orbital fissure; gCNV3, groove for root of CN V3 and semilunar ganglion; hpf, hypophyseal fossa; iss, presphenoid surface of intersphenoidal synchondrosis; jgs, jugum sphenoidale; mlp, medial lamina of pterygoid process of palatine; opc, optic canal; ors, orbitosphenoid; pcp, posterior clinoid process; prc, presphenoid corpus; ptf, pterygoid fossa; sch, sulcus chiasmatis; sps, sphenoidal sinus; spv, sphenopalatine vacuity; sr, sphenoidal recess; tcf, transverse canal foramina. Scale bar = 5 mm.

and forms the posterior extension of the medial margin of the pyramidal process of the palatine. Its medial surface forms the posterolateral surface of the nasopharyngeal duct. Posteroventrally, the medial lamina terminates with a pointed hamular process. The lateral lamina [=ectopterygoid crest of Wible (2007)] extends anteroventrally from the lateral part of the basisphenoid and tapers anteriorly into a rugose apex, which

inserts into a fissure in the pyramidal process of the palatine. The lateral lamina of the pterygoid does not extend as far posteriorly as the medial lamina, which is similar to the condition present in ochotonids and leporids (contra Dice, 1933; Wible, 2007, char. 37). The medial and lateral laminae of the pterygoids form the posteromedial and anterolateral boundaries of the pterygoid fossa, respectively.



## Squamosal

The squamosal occupies the lateral part of the braincase and forms the lateral surface of the middle cranial fossa, internally. It comprises the squama of the squamosal and an anterolaterally projecting zygomatic process. The posterior portion of the zygomatic process contributes to the cranial part of the craniomandibular joint. In FMNH PM9476, the squamosals are incompletely preserved; the left squamosal is preserved partially, with the anterior portion of the zygomatic process broken, whereas the right squamosal is represented only by its zygomatic process (Figures 3A,B, 8). The morphology of the squamosal in *P. haydeni* is somewhat intermediate between the squamosal of leporids, which is approximately quadrangular in outline in lateral view, and the dorsoventrally narrow squamosal present in ochotonids (Krause, 1884; Craigie, 1948; Wible, 2007). Anteriorly, the squama of the squamosal projects medially onto the orbital wall, where it contacts the frontal, dorsally, and the orbitosphenoid, ventrally. Dorsally, the main portion of the squamosal forms a weakly interdigitating suture with the parietal, whereas ventrally it contacts the alisphenoid. In FMNH PM9476, the squama of the squamosal is perforated by a large, oval opening, but it is difficult to determine whether this opening is entirely artificial, or it represents indeed the postglenoid foramen enlarged as a result of damage.

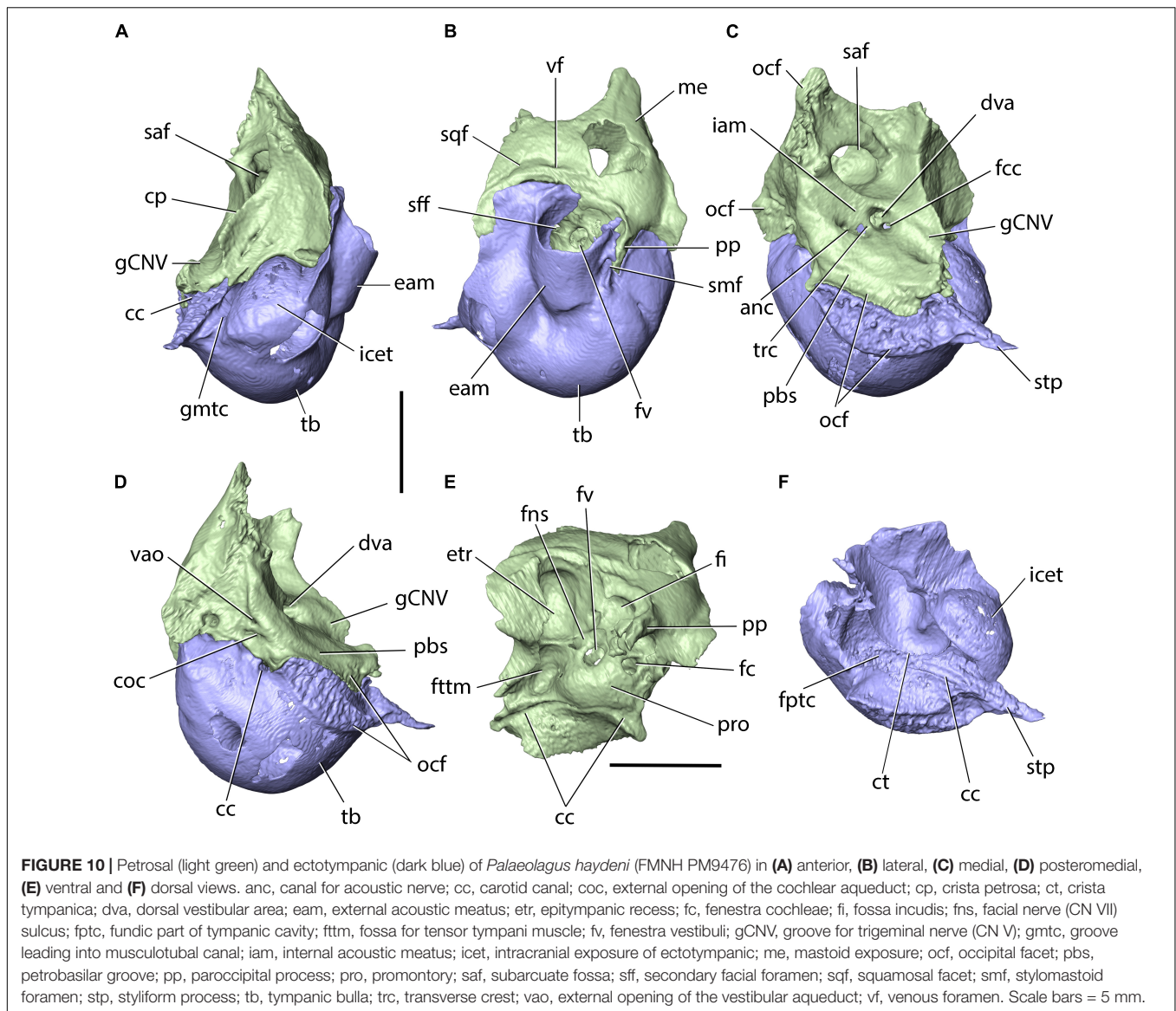
The zygomatic process forms a root which extends anteroventrolaterally, and an anterior portion which extends anteroventromedially. The root bears a prominent transverse ridge, anteroventrally, which separates the anteromedial surface of the squamosal from the concave glenoid cavity (mandibular fossa). The posterior surface of the root of the zygomatic process, together with part of the ventrolateral surface of the squama, form the temporal fossa, which is demarcated dorsally by a prominent, sub-longitudinal ridge, located dorsally to the mentioned large opening (postglenoid foramen). The anteroventral portion of the zygomatic process is triangular

in outline in lateral view, mediolaterally flattened and laterally concave. Ventrally, it forms a sharp crest, which inserts into a groove located on the posterodorsal margin of the zygomatic and the two bones form a straight, sub-longitudinal suture. The posterior portion of the squamosal is incompletely preserved in FMNH PM9476, but the mastoid portions of the petrosals of the specimen bear prominent facets for the posteroventral process of the squamosal, located anterodorsally to the dorsal margin of the external acoustic meatus (Figure 10B).

## Petrosal

The petrosal occupies the posterodorsolateral portion of the cranium and is approximately pyramidal in shape, with an anteromedially directed apex (Figure 10). On the dorsal surface, a prominent petrosal crest (=crista petrosa) extends from the apex, posterolaterally, and separates the cerebral and cerebellar surface of the petrosal into anterior and medial portions; it also separates the medial and posterior cranial fossae. The medial surface possesses a large, sub-oval opening of the subarcuate fossa, which houses the petrosal lobule of the cerebellum. Ventral to the subarcuate fossa, the medial surface bears the internal acoustic meatus, which is divided by the transverse crest into the anterodorsal opening of the facial canal and the posteroventral area occupied predominantly by the cochlear nerve. Anteroventral to the internal acoustic meatus, the petrosal bears an anteroposteriorly short and mediolaterally broad groove for the passage of the trigeminal nerve (CN V), which continues onto the dorsal surface of the basisphenoid. Ventromedially, the medial surface possesses a prominent petrobasilar sulcus for the ventral (inferior) petrosal sinus. Ventral to the petrobasilar sulcus, the petrosal is overlapped by the basilar portion of the occipital.

The posteromedial surface of the petrosal bears an approximately triangular articular surface for the occipital bone, demarcated anteromedially and posterodorsally by low



ridges. Immediately ventral to the anteromedial ridge, the petrosal bears the external opening for the vestibular aqueduct. Ventral to this opening, the petrosal produces a small, but deep cleft, containing the external opening of the cochlear aqueduct. The ventral portion of the posteromedial surface of the petrosal forms the anterolateral border of the jugular foramen.

The tympanic (ventral) surface of the petrosal forms the dorsal roof of the tympanic cavity. In its central portion, the tympanic surface bears an eminence, the promontory (=promontorium), which indicates the position of the basal turn of the cochlea situated immediately dorsally. Lateral to the promontory, the petrosal is perforated by the fenestra vestibuli (=vestibular [oval] window), which is closed by the footplate of the stapes in life. Posteromedial to the fenestra vestibuli, the petrosal bears the fenestra cochleae (=cochlear [round] window), which is closed by the secondary tympanic membrane in life. The tympanic surface also bears three distinct fossae: the fossa for the tensor

tympani muscle, located anteromedial to the fenestra vestibuli; the epitympanic recess, which lies dorsolaterally to the tensor tympani fossa and is occupied by the incus and the head of the malleus in life; and a fossa lying posteromedially to the fenestra cochleae, which represents the fossa incudis for the short process (=crus breve) of the incus. A sulcus representing the dorsal portion of the carotid canal is also present in the tympanic surface. The sulcus extends anterolaterally from a notch representing the dorsal portion of the posterior carotid foramen. On the lateral surface of the promontory, the sulcus changes its orientation to anteroventral and extends toward the carotid groove on the dorsal surface of the basisphenoid.

The lateral surface of the petrosal was partly overlapped by the thin, posteroventral process of the squamosal, as indicated by the presence of a dedicated, squamosal facet, and the extent of the squamosal in more complete skulls (Figure 2; see also Wood, 1940, pl. XXXIV, Figure 2). This condition

resembles Leporidae (Wible, 2007), although the posteroventral process of the squamosal is shorter in *Palaeolagus* than in extant leporids. The lateral exposure of the mastoid portion in *P. haydeni* is more extensive than in leporids, but most probably the posteroventral process of the squamosal separated the dorsal side of the tympanic bulla and the mastoid, as in Leporidae. The surface of the mastoid exposure is smooth, a feature *P. haydeni* shares with ochotonids, whereas in leporids the mastoid exposure is extensively pitted (Wible, 2007). The mastoid exposure forms a prominent mastoid (paroccipital) process, which inserts into a fissure located in the dorsal surface of the ectotympanic and forms the posterior boundary of the stylomastoid foramen, through which the facial nerve (CN VII) leaves the petrosal. The mastoid process is shorter in *Palaeolagus* than in leporids, displaying a somewhat intermediate morphology between ochotonids and leporids.

## Ectotympanic

The ectotympanic is located in the posteroventrolateral portion of the cranium and forms the greatly expanded tympanic bulla (Figures 3A,B,D–F, 10A–D,F). Laterally, the ectotympanic bears the osseous external acoustic meatus, which has the form of a posterolaterally directed canal leading from the external ear to the tympanic membrane, and resembles the external acoustic meatus of leporids, but differs markedly from the short, laterally directed meatus in ochotonids (Wible, 2007, char. 26). Posterior to the external acoustic meatus, the dorsal surface of the ectotympanic forms a fissure for the mastoid process. Ventromedially, the external acoustic meatus terminates with the crista tympani, which in life forms the base of the tympanic membrane.

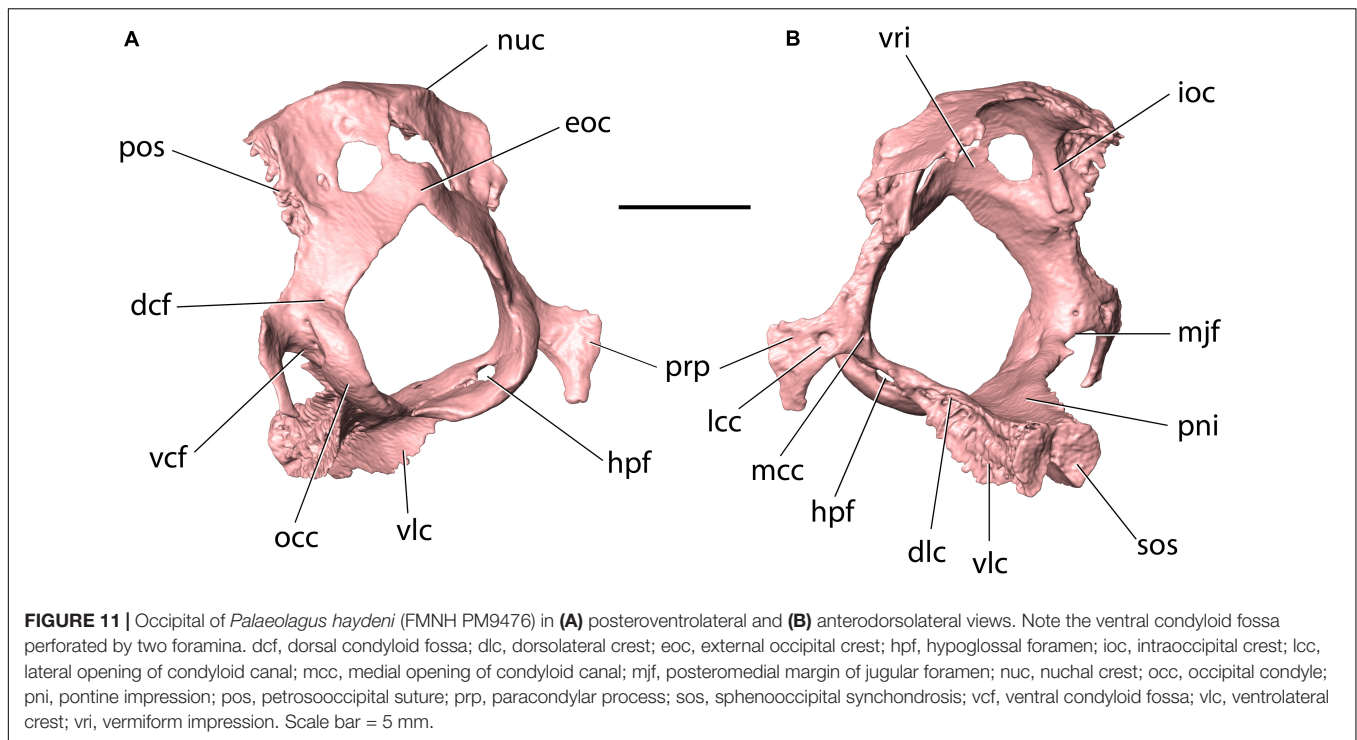
Anteromedially, the ectotympanic forms an oblique styloform process which underlaps the basisphenoid. Immediately lateral to the styloform process, the tympanic forms the musculotubal canal, which is occupied by the eustachian tube in life and forms a connection between the middle ear and the nasopharynx. Following Evans and de Lahunta (2013), the tympanic cavity can be divided into three parts: the fundic part, which is the largest and most ventrally positioned; the proper tympanic cavity, located opposite the tympanic membrane; and a dorsal part for the incus, part of the stapes and head of the malleus, formed by the eptympanic recess. The carotid canal for the internal carotid artery (ICA) is located entirely between the petrosal and tympanic, which form their dorsal and ventral portions, respectively. The carotid canal opens posteriorly with the posterior carotid foramen located anteroventrolaterally to the jugular foramen in the petrobasilar fissure. It then extends anterolaterally toward the medial surface of the promontory, where the orientation of the canal changes to anteromedial. The carotid canal opens toward the middle cranial fossa via the internal carotid foramen, located medial to the styloform process. The ICA position in *P. haydeni* differs from that in extant lagomorphs. In ochotonids, the ICA is more medial and it enters the middle cranial fossa via a carotid notch. In leporids, on the other hand, the carotid canal is present, but is located within the wall of the ectotympanic, posteriorly, and is bordered by the petrosal and ectotympanic only anteriorly (Meng, 1991; Wible, 2007, char. 44). An anterodorsal portion of the wall of

the tympanic bulla is exposed in the middle cranial fossa in *P. haydeni*, in contrast to extant lagomorphs (Meng, 1991).

## Occipital

The occipital occupies the posterior portion of the cranium and forms a bony ring around the foramen magnum (Figure 11). The occipital comprises four portions: the ventral, unpaired basilar portion (basioccipital), the paired lateral portions (exoccipitals) and the unpaired, dorsal squamous portion (supraoccipital). All four portions develop as separate ossifications and fuse into a single occipital bone during ontogeny (Craigie, 1948).

The basilar portion (basioccipital) occupies the posterior portion of the cranial base. It is mediolaterally narrowest anteriorly, and its mediolateral width increases posteriorly toward the foramen magnum. In this respect, the basioccipital of *P. haydeni* resembles that in *Rhombomylus*, *Gomphos*, *Prolagus*, and *Ochotona*, but differs from the basioccipital in leporids, which is mediolaterally broadest anteriorly (Wible, 2007, char. 45). The dorsal surface of the basioccipital is exposed in the ventral part of the posterior cranial fossa and bears an anteroposteriorly elongate pontine impression. Posteroventrally, the basioccipital bears a subtle, median ridge (compare with Dice, 1933, Figure 2). A similar median ridge is also present in *Rhombomylus* (Meng et al., 2003, Figure 33), *Gomphos* (Asher et al., 2005, Figure 2), leporids and *Ochotona* (Wible, 2007, Figure 4), but whereas it is also weakly developed in leporids, *Rhombomylus*, and *Gomphos*, it is much more prominent in *Ochotona* and extends further anteriorly. In addition, lateral to the median ridge, the ventral surface of the basioccipital forms prominent grooves for the rectus capitis anterior in leporids and *Ochotona* (Wible, 2007), which are only weakly developed in *P. haydeni*. Anteriorly, the basioccipital bears a transverse, rugose articular surface, which is appressed against a similar surface located on the basisphenoid corpus, with both surfaces comprising the sphenoccipital synchondrosis. The lateral surface of the basioccipital gives rise to two pairs of crests: a dorsolateral pair and a ventrolateral pair (=tympanic processes of Wible, 2007). The oblique lateral surfaces of these crests are rugose and whereas the anterolateral crests overlap the medial surfaces of the petrosals, immediately ventral to the petrobasilar groove, the ventrolateral crests overlap the tympanic bones, medially, and contribute to the medial walls of the tympanic bullae. In leporids, the tympanic crests are oriented dorsally and laterally, instead of dorsolaterally and ventrolaterally. Furthermore, the dorsal crest does not overlap the medial surface of the petrosal, but abuts against its medial margin, and the ventrolateral crest does not overlap the tympanic bulla, but contacts an articular surface that is separated from the bulla by a deep groove (*O. cuniculus*, ZPAL comparative collection). In *Ochotona*, the ventromedial crests overlap the medial walls of the tympanic bullae as in *P. haydeni*, but the exact morphology of the dorsal or dorsolateral crests is unknown (Wible, 2007, char. 46). Posterolaterally, the basioccipital forms the ventral portions of the occipital condyles, whereas posteriorly it bears a sharp, concave posterior margin, which forms the intercondylar notch and the ventral margin of the foramen magnum. Immediately anterior to the intercondylar notch, the ventral surface of the



basioccipital bears a small pharyngeal tubercle in *O. cuniculus* (ZPAL, comparative collection), which is absent in *P. haydeni* and *Ochotona*.

The paired lateral portions (exoccipitals) form the lateral margins of the foramen magnum and bear the main parts of the occipital condyles. Lateral to the dorsal portion of the occipital condyle, the exoccipital forms a slender paracondylar (=jugular, =paramastoid) process, which extends ventrolaterally, and then ventromedially. This resembles the condition in leporids, but differs from *Ochotona*, in which the paracondylar process extends ventrolaterally and is much broader (Wible, 2007, Figure 4). The paracondylar process in *P. haydeni* is anteroposteriorly compressed, has a convex anterior surface and a concave posterior surface and extends about halfway down the tympanic bulla, like in *Ochotona*, but unlike leporids, in which the paracondylar process extends almost along the entire dorsoventral height of the bulla (Wible, 2007, char. 29). The paracondylar process in *P. haydeni* is widely separated from the paroccipital process of the mastoid by the posterior surface of the tympanic (contra Wible, 2007, char. 30). A similar condition is present in *Ochotona*, but differs from the condition in leporids, in which both processes almost abut against each other, ventrally (Wible, 2007, char. 30). The anterior surface of the paracondylar process bears two foramina, possibly representing the external openings of the condyloid canal – a larger, lateral foramen and a smaller, medial foramen (compare with Evans and de Lahunta, 2013, p. 89). The anterior surface of the paracondylar process is pressed against the posteromedial surface of the petrosal and the posterodorsal surface of the tympanic bulla. A small, pointed process extends anterolaterally from the base of the paracondylar process, so that the concave margin of

the exoccipital between them forms the posteromedial margin of the jugular foramen, bound anterolaterally by the petrosal. Between the dorsal portion of the occipital condyle and the paracondylar process, the exoccipital forms a ventral condyloid fossa, perforated by a pair of ventral condyloid foramina on each side. The presence of ventral condyloid foramina is variable in *Ochotona* and within Leporidae (Wible, 2007, char. 48). The exoccipital also bears a dorsal condyloid fossa, which does not bear any foramina. This resembles the condition in *Ochotona* and some leporids, but differs from *Lepus* and *Oryctolagus*, in which the dorsal condyloid fossa bears numerous small foramina (Wible, 2007, char. 49). Posteromedial to the jugular foramen, the exoccipital is perforated by a single hypoglossal foramen, like in *Ochotona*, *Gomphos*, and *Rhombomylus*. This is in contrast to the condition in leporids, in which the exoccipital bears two hypoglossal foramina (Wible, 2007, char. 47).

The squamous part (supraoccipital) forms the dorsolateral borders of the foramen magnum. It comprises a posteriorly convex, anteroventrally flattened sheet of bone, which bifurcates ventrally to fuse with the dorsal part of each exoccipital. Laterally, the supraoccipital forms an interdigitating suture with the posteromedial surface of the petrosal. At the intersection of the skull roof and the posterior cranial wall, the supraoccipital produces a prominent nuchal crest. Anterior to the nuchal crest, it forms an anteroposteriorly narrow dorsal exposure. Between the nuchal crest and the dorsal apex of the foramen magnum, a weakly developed external occipital crest is present. In all these respects, the supraoccipital of *P. haydeni* is remarkably similar to that in *Ochotona*. However, it differs markedly from the supraoccipital in leporids, in which it forms: (1) a nuchal crest well anterior to the intersection of the skull roof and posterior

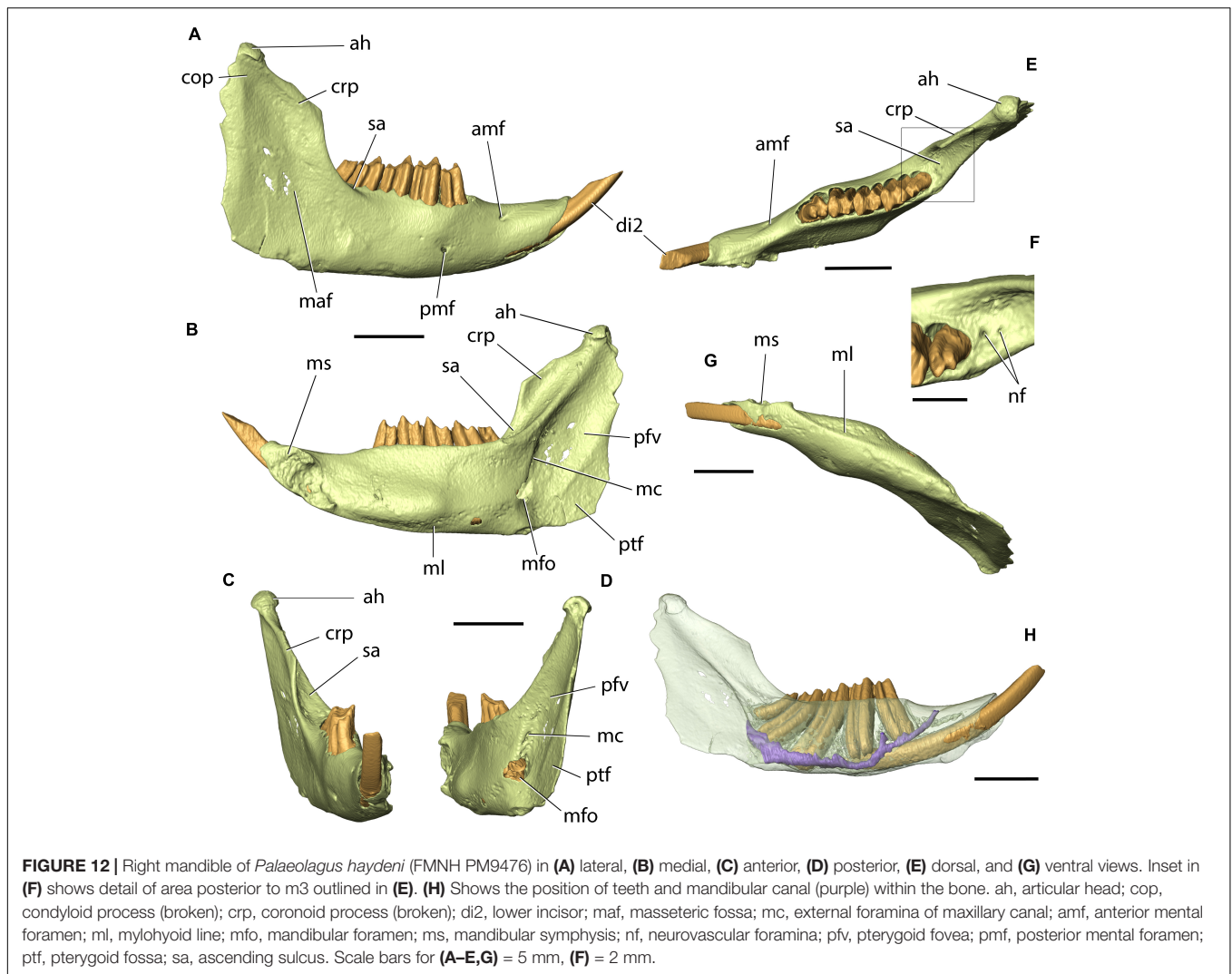


**FIGURE 12** | Right mandible of *Palaeolagus haydeni* (FMNH PM9476) in (A) lateral, (B) medial, (C) anterior, (D) posterior, (E) dorsal, and (G) ventral views. Inset in (F) shows detail of area posterior to m3 outlined in (E). (H) Shows the position of teeth and mandibular canal (purple) within the bone. ah, articular head; cop, condyloid process (broken); crp, coronoid process (broken); di2, lower incisor; maf, masseteric fossa; mc, external foramina of maxillary canal; amf, anterior mental foramen; ml, mylohyoid line; mfo, mandibular foramen; ms, mandibular symphysis; nf, neurovascular foramina; pfv, pterygoid fovea; pmf, posterior mental foramen; ptf, pterygoid fossa; sa, ascending sulcus. Scale bars for (A–E,G) = 5 mm, (F) = 2 mm.

cranial wall; (2) an extensive exposure on the dorsal surface of the skull; and (3) a prominent external occipital protuberance extending posteriorly to the nuchal crest (Wible, 2007, char. 7). The external surface of the supraoccipital is smooth in *P. haydeni*, and differs from both ochotonids, in which the external surface of the supraoccipital bears only a minute, single neurovascular foramen, dorsally, and from leporids, in which the surface is extensively pitted (Wible, 2007). The internal surface of the supraoccipital forms a concave vermiform impression, bounded laterally by prominent, internal occipital crests.

The foramen magnum, located within the occipital, comprises the passageway through which the medulla oblongata leaves the cranial fossa to form the spinal cord. The foramen magnum in *P. haydeni* differs from that in other lagomorphs in that it is approximately sub-circular in outline, and produces a pointed, dorsal apex. In contrast, in ochotonids and leporids, the foramen magnum forms a round, dorsal apex, and the supraoccipital also bears a pair of prominent nuchal tubercles, ventromedially, which give the foramen magnum a pentagonal outline (Wible, 2007, Figure 4).

## Mandible

The mandible is well-preserved in FMNH PM9476, except for the posterior portions of both mandibular rami and the right coronoid process, which are broken (Figure 12; compare with Figures 2E,F).

The mandible is formed by two hemimandibles joined anteriorly at the mandibular symphysis. Each hemimandible comprises a horizontal portion and an approximately perpendicular mandibular ramus. The horizontal portions of both contralateral hemimandibles form the body (corpus) of the mandible. Anteriorly, the body of the mandible lies in a sagittal plane, and becomes obliquely oriented posterior to the mandibular symphysis, so that both contralateral mandibular bodies form an angle of approximately 40°. Anteriorly, the mandibular body bears the alveolus for di2. Posteriorly, the dorsal surface of the mandibular body bears alveoli for p3–p4 and m1–m3, which are approximately equal in size, except for the alveolus for m3, which is markedly smaller. Posterior to the di2 alveolus, and anterior to the p3 alveolus, the dorsal surface of the mandibular body is concave and

contributes to the ventral part of the diastema. There are two mental foramina in each mandibular body: an anterior mental foramen, located approximately at the posterior one-third of the anteroposterior length of the diastema, which is likely homologous with the mental foramen in leporids located in a similar position, and a posterior mental foramen, placed below the posterior part of p3, likely homologous with the more posteriorly placed (m3 level) mental foramen present in ochotonids (Wible, 2007). Ventrally, the mandibular body bears a prominent mylohyoid line for the insertion of the mylohyoid muscle.

The lateral surface of the mandibular ramus is concave and forms an extensive masseteric fossa. Anteroventrally to the masseteric fossa, the mandibular ramus bears a tuberosity, which is only slightly demarcated in FMNH PM9476, but is much more prominent in other specimens of *P. haydeni* (Figure 2F; see also Troxell, 1921; Wood, 1940). The medial surface of the mandibular ramus bears two depressions: an anterodorsal pterygoid fovea, which marks the attachment site for the lateral pterygoid muscle, and a posteroventral pterygoid fossa, for the insertion of the medial pterygoid muscle. Both depressions are separated from each other by a weakly demarcated, oblique ridge, which is also present in extant leporids, but is absent in ochotonids (Wible, 2007, char. 57). Anteromedially, a prominent, oblique ridge separates the pterygoid fovea from the anteromedial surface of the mandibular ramus [=sulcus ascendens of Krause (1884)]. Posterior to m3, the anteromedial surface of the mandibular ramus is perforated by a single (left side) or two (right side) minute foramina. Posterodorsally to the mylohyoid line, the mandibular ramus bears a mandibular foramen, which is located at a level below the mandibular tooth row (contra Asher et al., 2005, char. 48). Dorsal to the mandibular foramen, the medial surface of the mandibular ramus is perforated by a minute foramen, possibly representing the posterior opening of the maxillary canal. Anterodorsally, the mandibular ramus bears a prominent, dorsomedially directed coronoid process, which is much more prominent than the coronoid process present in extant lagomorphs (Figures 2E,F). The condylar processes in FMNH PM9476 are broken posteriorly, but preserve the prominent articular heads, which extend posteriorly into a mediolaterally narrow crest in more complete specimens (Figures 2E,F). Posteroventrally, the mandibular ramus produces an anteroposteriorly elongate angular process, which has a convex ventral margin, a concave dorsal margin and tapers to a point, posteriorly. A prominent masseteric line extends from the ventrolateral surface of the angular process onto the lateral surface of the angular process, resembling the prominent masseteric line in leporids, but differing markedly from the masseteric line in ochotonids, which is restricted to the ventrolateral surface of the angular process (Wible, 2007). The extent of the pterygoid shelf on the medial surface of the angular process is difficult to determine in the specimens of *P. haydeni* examined in this study because of incomplete preservation, but seems to be restricted to the posteroventral portion of the mandible, as in ochotonids, unlike the anteroposteriorly elongate pterygoid shelf present in extant leporids (Wible, 2007, char. 59).

The mandibular canal opens posteriorly at the mandibular foramen and extends anteriorly below the roots of m1–m3. It then extends ventromedially to the root of p4, and continues anterodorsally, lying ventral to the root of p3. The mandibular canal opens anteriorly at the anterior mental foramen. The mandibular canal also forms a mediolaterally short, lateral branch located between the p3 and p4 alveoli, which opens laterally at the posterior mental foramen.

## DISCUSSION

There are only few contributions that treated the cranial morphology of fossil lagomorphs in some detail. Among them, Wood (1940), Dawson (1958), and Fostowicz-Frelik (2013) concern North American Paleogene lagomorphs, in particular *Palaeolagus* (Wood, 1940; Dawson, 1958) or closely related genera (Fostowicz-Frelik, 2013). Other works covered mostly Neogene fossil ochotonids: *Alloptox* (Wu, 2003), *Austrolagomys* (= *Kenyallagomys* in MacInnes, 1953), and *Prolagus* (Dawson, 1969).

Ever since Dice (1929), *Palaeolagus* was recognized as belonging to Leporidae on the basis of the dentition, mandible, and muzzle morphology, the parts most frequently preserved in the fossil record (Dice, 1933; Wood, 1940; Dawson, 1958). However, recent phylogenetic studies of lagomorphs and Glires have, in general, supported the position of *Palaeolagus* as a stem lagomorph (Asher et al., 2005; Wible, 2007; Fostowicz-Frelik and Meng, 2013; Lopatin and Averianov, 2020).

Thus, the current study aimed at the reappraisal of the cranial morphology of *P. haydeni* in order to provide new morphological data as a base for deciding between the two phylogenetic hypotheses. Micro-CT scanning allowed us to study the internal cranial structures and scrutinize the whole skull, bone by bone, comparing it with the crown taxa in detail, using Wible's (2007) character matrix as the basis for our comparisons. Our study of *Palaeolagus* revealed that its cranial morphology shares characters not only with extant leporids but also with *Ochotona* (Table 1). Out of 46 characters analyzed by us, in 21 *Palaeolagus* showed features characteristic of extant Leporidae, in 13 the features characteristic of Ochotonidae (represented by *Ochotona* and *Prolagus*) and in seven, shared with both clades. However, in five characters *Palaeolagus* displayed morphology unlike any of the crown groups of Lagomorpha. These were: the morphology of the orbital process of maxilla, which is elongated in *Palaeolagus*, the absence of the zygomatico-orbital canal, a broader posterior squamosal, the absence of piriform fenestra, and the presence of two mental foramina (Table 1). This last combination of features can be viewed as plesiomorphic for all Glires, because *Palaeolagus* shares them with *Rhombomylus* (see Meng et al., 2003; Wible, 2007), a basal gliroid mammal which is neither a lagomorph nor a rodent (Asher et al., 2005).

The skull of *P. haydeni* shows a leporid-like structure of the muzzle, including the nasals, premaxilla–maxilla articulation, frontals with nascent postorbital processes, as well as the most part of the maxilla, showing extended lateral fenestration and leporid-like arrangement of the alveolar processes. Furthermore,

**TABLE 1** | Comparison of cranial character states based mostly on the character-taxon matrix of Wible (2007), between Ochotonidae (represented by *Ochotona* and *Prolagus*), Leporidae [represented by sample studied by Wible (2007) and the comparative material for the present study], and *Palaeolagus haydeni*.

No.	Character	Ochotonidae	Leporidae	<i>Palaeolagus haydeni</i>
1	Shape of the nasals	*Narrow posteriorly and expanded anteriorly or narrow with sides parallel	Broad posteriorly, with V-shaped frontal articulation	Broad posteriorly, with V-shaped frontal articulation
2	Dorsal margin of the premaxilla	Smooth, convex	Dorsal extension well developed	Dorsal extension weak
3	Premaxilla/maxilla suture	Premaxilla wedges into maxilla	Maxilla wedges into premaxilla	Maxilla wedges into premaxilla
4	Postorbital process	Absent	Present	Present
5	Supraorbital notch	Absent	Present	Absent
6	Braincase pitting	Absent	Present	Absent
7	External occipital protuberance and nuchal crest	Does not dominate dorsal occiput; nuchal crest absent	Dominates dorsal occiput; nuchal crest present	Does not dominate dorsal occiput; nuchal crest absent
8	Maxillary fenestra, pars facialis	Single, large opening	Numerous, small openings	Numerous, small openings
9	Maxillary fenestra, pars orbitalis	Present	Absent	Present
10	Lacrimal facial process	Reduced	Reduced, but with pointed lacrimal tubercle	Reduced, but with pointed lacrimal tubercle
11	Position of nasolacrimal canal	Lateral to incisor	Position not related to incisor	*Position not related to incisor
12	Anteroventral orbital rim	Round	Square	Square
13	Sphenopalatine foramen	Between the palatine and maxilla	Within the palatine	*Between the palatine and maxilla
14	'Orbital process' of maxilla	Narrow	Narrow	*Elongated anteroposteriorly
15	Alveolar process of maxilla	Close to the lateral wall of the orbit	Close to the medial wall of the orbit	Close to the medial wall of the orbit
16	Root exposure in orbit wall	Absent	Present	Weakly present
17	Zygomatico-orbital canal	Present	Present	Absent
18	Masseteric crest	Short, formed as a pronounced tubercle	Long, extended along the ventrolateral margin of the anterior zygomatic root	Long, extended along the ventrolateral margin of the anterior zygomatic root
19	Posterior process of zygomatic	Substantially elongated	Present, but not very long (with rounded tip)	Present, but not very long (with rounded tip)
20	Posterior squamosal	Long and narrow	Narrow with processes squamosum	Broader but with posterior process external to the acoustic meatus
21	External acoustic meatus	Tube very short and laterally directed	Tube elongate and posterolaterally directed	Tube elongate and posterolaterally directed
22	Lateral exposure of mastoid	Present, immediately dorsal to external acoustic meatus	Present, immediately dorsal to external acoustic meatus	*Present, dorsal to the acoustic meatus
23	Paracondylar process	Short, extends not longer than a halfway down posterior bullar wall	Long, extends halfway or completely down posterior bullar wall	*Intermediate, extends halfway down posterior bullar wall
24	Paroccipital and paracondylar process relationship	Distant	Close, (approximating)	*Distant
25	Incisive foramen	Elongated and partitioned into two openings; posteriorly at the level of P4	Elongated, single; posteriorly reaching P2	Elongated, single, reaching P2 or P2/P3 alveolar septum
26	Major palatine foramen	Multiple openings in palatine	Single opening within palatine or between palatine and maxilla	Single opening within palatine
27	Premolar foramen	Present	Absent (generally)	Absent
28	Posterior palate	Level with M1	Level with M1	Level with M1/M2
29	Sphenopalatine vacuity	Present, near midline	Absent or present, near midline, or present, laterally positioned	*Present, near midline
30	Ento- and ectopterygoid crests	Ectopterygoid crest of variable length in relation to the entopterygoid crest; shorter ( <i>Ochotona</i> ) or longer ( <i>Prolagus</i> ); ends anterior or posterior to the entopterygoid crest, respectively	Ectopterygoid crest shorter, ends anterior to the entopterygoid crest	*Ectopterygoid crest short, ends anterior to the entopterygoid crest
31	Foramen ovale	Placed within alisphenoid or between alisphenoid and petrosal	Placed between alisphenoid and petrosal	Placed within alisphenoid
32	Piriform fenestra anterior to auditory bulla	Present	Present	Absent

(Continued)

TABLE 1 | Continued

No.	Character	Ochotonidae	Leporidae	<i>Palaeolagus haydeni</i>
33	Craniopharyngeal canal	Absent	Present	Present
34	Carotid canal	Absent	Present	Present
35	Basioccipital	Long, broadens posteriorly	Short, broadest anteriorly	Long, broadens posteriorly
36	Lateral margin of the basioccipital	Bearing prominent tympanic process overlapping medial wall of auditory bulla	With thick, flattened prominence meeting the downturned lip from the auditory bulla	Bearing prominent tympanic process overlapping medial wall of auditory bulla
37	Hypoglossal foramen	One	Two or more	One
38	Ventral condyloid foramen	Present or absent	Present or absent	Present
39	Dorsal condyloid foramen	Absent	Present or absent	Absent
40	Number of mental foramina	One	One	*Two
41	Anterior most position of mental foramen	At the level of ultimate molar	At the back of diastema	The anterior one at the back of diastema
42	Masseteric line	Restricted posteriorly on ramus	Along ventral margin of the mandibular ramus	Along ventral margin of mandibular ramus
43	Maxillary canal	Present	Present	*Probably present
44	Mandibular foramen	Inferior to occlusal surface of tooth row	Inferior to occlusal surface of tooth row	*Inferior to occlusal surface of tooth row
45	Pterygoid fovea	Not delineated	Prominently delineated	*Prominently delineated
46	Pterygoid shelf	Restricted posteriorly on ramus	Along ventral margin of mandibular ramus	*Restricted posteriorly on the ramus

Asterisk denotes modified character state change from that in Wible (2007).

the structure of the zygomatic root of the maxilla and the zygomatic are typical of leporids. The ochotonid features can be found in the basicranium and, generally, in the posterior part of the skull (Table 1). The basioccipital is ochotonid-like in having the tympanic processes encroaching the wall of the auditory bullae; furthermore, the structure of the petrosal mastoid exposure is more ochotonid-like than leporid-like, although its condition is overall intermediate. The posterior part of the skull with the relatively level parietals and lack of the nuchal crest at the occipital also resembles more that of *Ochotona* than of any modern leporid.

The described cranial characters of *Palaeolagus* are not characteristic of only one of the crown clades; thus, this lagomorph is better considered as a stem lagomorph. Its apparent mosaic morphology has at least two important implications. First, the fact that the early lagomorph *Palaeolagus*, which does not have an immediate relationship to either of the crown clades, exhibits a mixture of morphological characters typically associated either with ochotonids or leporids, indicates its independent position, already suggested by Fostowicz-Frelik and Meng (2013). Second, it allows us to assume that some of the cranial characters observed in extant taxa and regarded thus far as synapomorphies for the recent clades are most likely plesiomorphic.

The *Palaeolagus* lineage most probably originated in the late middle Eocene (see Fostowicz-Frelik and Tabrum, 2009), and it was already well represented in the early late Eocene (Dawson, 2008). Therefore, the skull of *Palaeolagus haydeni* is a very good reference point for advanced stem lagomorphs, which most probably gave rise to Leporidae in North America (see Fostowicz-Frelik, 2013). However, to reconstruct the ancestral cranial morphotype of Ochotonidae more data is needed from

the Eocene Asian taxa, of which our knowledge is at present very fragmentary.

## DATA AVAILABILITY STATEMENT

The original contributions presented in the study are included in the article/Supplementary Material, further inquiries can be directed to the corresponding author/s.

## AUTHOR CONTRIBUTIONS

ŁF-F designed the study. AW processed and visualized the CT-data. Both authors analyzed the data, wrote the manuscript, and approved the final version.

## FUNDING

This research was funded by National Science Centre (Cracow, Poland) grant number 2015/18/E/NZ8/00637, a visiting scholarship from FMNH, and an AMNH Roosevelt Research Fellowship to ŁF-F.

## ACKNOWLEDGMENTS

We are grateful to W. Simpson (FMNH) and R. J. Emry (USNM) for access to the *Palaeolagus* specimens and to M. Hill (AMNH) for CT-scanning the FMNH PM9476 skull. The senior author is especially indebted to J. Meng (AMNH) for valuable discussions, support for this study, and access

to the AMNH *Palaeolagus* material. We thank F. Ippolito (previously AMNH) for the photos of the skulls used in **Figures 1, 2**. A. Kapuścińska (ZPAL) kindly created a visualization of the head of *Palaeolagus*, and A. Hołda-Michalska (ZPAL) helped us edit **Figures 1, 2**.

## REFERENCES

- Asher, R. J., Meng, J., Wible, J. R., McKenna, M. C., Rougier, G. W., Dashzeveg, D., et al. (2005). Stem Lagomorpha and the antiquity of Glires. *Science* 307, 1091–1094. doi: 10.1126/science.1107808
- Asher, R. J., Smith, M. R., Rankin, A., and Emry, R. J. (2019). Congruence, fossils and the evolutionary tree of rodents and lagomorphs. *R. Soc. Open Sci.* 6:190387. doi: 10.1098/rsos.190387
- Craigie, E. H. (1948). *Bensley's Practical Anatomy of the Rabbit: An Elementary Laboratory Text-Book in Mammalian Anatomy*, 8th Edn. Toronto, ONT: University of Toronto Press.
- Dawson, M. R. (1958). Later Tertiary Leporidae of North America. *Univ. Kansas Paleontol. Contrib. Vertebrata* 6, 1–75.
- Dawson, M. R. (1969). Osteology of *Prolagus sardus*, a Quaternary ochotonid (Mammalia: Lagomorpha). *Palaeovertebrata* 2, 157–190. doi: 10.18563/pv.2.4.157-190
- Dawson, M. R. (2008). “Lagomorpha,” in *Evolution of Tertiary Mammals of North America*, Vol. 2, eds C. M. Janis, G. F. Gunnell, and M. D. Uhen, (Cambridge: Cambridge University Press), 293–310.
- Dice, L. R. (1929). The phylogeny of the Leporidae, with description of a new genus. *J. Mammal.* 10, 340–344. doi: 10.2307/1374124
- Dice, L. R. (1933). Some characters of the skull and skeleton of the fossil hare, *Palaeolagus haydeni*. *Papers Mich. Acad. Sci. Art. Lett.* 18, 301–306.
- Evans, H. E., and de Lahunta, A. (2013). *Miller's Anatomy of the Dog*. St. Louis, MO: Elsevier-Saunders.
- Fostowicz-Frelik, Ł. (2013). Reassessment of *Chadrolagus* and *Litolagus* (Mammalia: Lagomorpha) and a new genus of North American Eocene lagomorph from Wyoming. *Am. Mus. Novit.* 3773, 1–76. doi: 10.1206/3773.2
- Fostowicz-Frelik, Ł. (2017). “Convergent and parallel evolution in early Glires (Mammalia)” in *Evolutionary Biology: Self/Nonsel Evolution, Species and Complex Traits Evolution, Methods and Concepts*, ed. P. Pontarotti, (Cham: Springer), 199–216. doi: 10.1007/978-3-319-61569-1\_11
- Fostowicz-Frelik, Ł., Frelik, G. J., and Gasparik, M. (2010). Morphological phylogeny of pikas (Lagomorpha: *Ochotona*), with a description of a new species from the Pliocene/Pleistocene transition of Hungary. *Proc. Acad. Nat. Sci. Phila.* 159, 97–118. doi: 10.1635/053.159.0107
- Fostowicz-Frelik, Ł., Li, C.-K., Li, Q., Meng, J., and Wang, Y.-Q. (2015). *Strenulagus* (Mammalia: Lagomorpha) from the middle Eocene Irind Manha Formation of the Erlan Basin, Nei Mongol, China. *Acta Geol. Sin. (Eng. Ed.)* 89, 12–26. doi: 10.1111/1755-6724.12391
- Fostowicz-Frelik, Ł., and Meng, J. (2013). Comparative morphology of premolar foramen in lagomorphs (Mammalia: Glires) and its functional and phylogenetic implications. *PLoS One* 8:e79794. doi: 10.1371/journal.pone.0079794
- Fostowicz-Frelik, Ł., and Tabrum, A. R. (2009). Leporidae (Mammalia, Lagomorpha) from the Diamond O Ranch local fauna, latest middle Eocene of southwestern Montana. *Ann. Carnegie Mus.* 78, 253–271. doi: 10.2992/007.078.0303
- Fostowicz-Frelik, Ł., and Wolniewicz, A. S. (2021). CT-informed skull osteology of *Palaeolagus haydeni* (Mammalia: Lagomorpha). *Dryad Dataset*. doi: 10.5061/dryad.crdjfn338
- Frahnert, S. (1999). Morphology and evolution of the Glires rostral cranium. *Mitt. Mus. Nat. Berlin* 75, 229–246. doi: 10.1002/mmnz.19990750205
- Ge, D., Yao, L., Xia, L., Zhang, Z., and Yang, Q. (2015). Geometric morphometric analysis of skull morphology reveals loss of phylogenetic signal at the generic level in extant lagomorphs (Mammalia: Lagomorpha). *Contrib. Zool.* 84, 267–284. doi: 10.1163/18759866-08404001
- Insom, E., Magnoni, M. L., and Simonetta, A. M. (1990). Etudes sur la morphologie évolutive des Ochotonidés (Mammalia, Lagomorpha). 1. La morphologie crânienne d'*Ochotona rufescens* et d'*Ochotona roylei*. *Mammalia* 54, 633–651.
- Koby, F. E. (1959). Contribution au diagnostic ostéologique différentiel de *Lepus timidus* Linné et *L. europaeus* Pallas. *Ver. Nat. Gesell. Basel* 70, 1–44.
- Krause, W. (1884). *Die Anatomie des Kaninchens in Topographischer und Operativer Rücksicht*. Leipzig: Wilhelm Engelmann.
- Li, C.-K., Meng, J., and Wang, Y.-Q. (2007). *Dawsonolagus antiquus*, a primitive lagomorph from the Eocene Arshanto Formation, Nei Mongol, China. *Bull. Carnegie Mus. Nat. Hist.* 39, 97–110. doi: 10.2992/0145-9058(2007)39[97:daapl]2.0.co;2
- Lopatin, A., and Averianov, A. (2020). *Arnebolagus*, the oldest eulagomorph, and phylogenetic relationships within the Eocene Eulagomorpha new clade (Mammalia, Duplicidentata). *J. Paleontol.* 1–12. doi: 10.1017/jpa.2020.94
- López-Torres, S., Bertrand, O. C., Lang, M. M., Silcox, M. T., and Fostowicz-Frelik, Ł. (2020). Cranial endocast of the stem lagomorph *Megalagus* and brain structure of basal Euarchontoglires. *Proc. R. Soc. B Biol. Sci.* 287:20200665. doi: 10.1098/rspb.2020.0665
- MacInnes, D. G. (1953). The Miocene and Pleistocene Lagomorpha of East Africa. *Foss. Mamm. Afr.* 6, 1–30.
- Meng, J. (1991). Ear features of *Palaeolagus* (Mammalia, Lagomorpha) and some character polarities. *J. Vertebr. Paleontol.* 11(Suppl. 3):47A.
- Meng, J., Hu, Y., and Li, C.-K. (2003). The osteology of *Rhombomylus* (Mammalia, Glires): implications for phylogeny and evolution of Glires. *Bull. Am. Mus. Nat. Hist.* 275, 1–247. doi: 10.1206/0003-0090(2003)275<0001:toormg>2.0.co;2
- Schneider, C. A., Rasband, W. S., and Eliceiri, K. W. (2012). NIH image to ImageJ: 25 years of image analysis. *Nat. Methods* 9, 671–675. doi: 10.1038/nmeth.2089
- Troxell, E. L. (1921). *Palaeolagus*, an extinct hare. *Am. J. Sci.* 1, 340–348. doi: 10.2475/ajs.s5-1.4.340
- Wahlert, J. H. (1974). The cranial foramina of protrogomorphous rodents, an anatomical and phylogenetic study. *Bull. Mus. Comp. Zool.* 146, 363–410.
- Wible, J. R. (2007). On the cranial osteology of the Lagomorpha. *Bull. Carnegie Mus. Nat. Hist.* 39, 213–234. doi: 10.2992/0145-9058(2007)39[213:otcoot]2.0.co;2
- Wible, J. R., and Shelley, S. L. (2020). Anatomy of petrosal and middle ear of the brown rat, *Rattus norvegicus* (Berkenhout, 1769) (Rodentia, Muridae). *Ann. Carnegie Mus.* 86, 1–35. doi: 10.2992/007.086.0101
- Wilson, D. E., Lacher, T. E., and Mittermeier, R. A. (eds) (2016). *Handbook of the Mammals of the World: Lagomorphs and Rodents I*. Barcelona: Lynx Edicions.
- Wood, A. E. (1940). The mammalian fauna of the White River Oligocene. Part III. Lagomorpha. *Trans. Am. Philos. Soc.* 28, 271–362. doi: 10.2307/1005524
- Wu, S.-Y. (2003). The cranial morphology and phylogenetic relationship of *Alloptox gobiensis* (Lagomorpha, Ochotonidae). *Vert. Palasiat.* 41, 115–130.

## SUPPLEMENTARY MATERIAL

The Supplementary Material for this article can be found online at: <https://www.frontiersin.org/articles/10.3389/fevo.2021.634757/full#supplementary-material>

**Conflict of Interest:** The authors declare that the research was conducted in the absence of any commercial or financial relationships that could be construed as a potential conflict of interest.

The reviewer, OB, declared a past co-authorship with one of the authors, ŁF-F, to the handling editor.

Copyright © 2021 Wolniewicz and Fostowicz-Frelik. This is an open-access article distributed under the terms of the Creative Commons Attribution License (CC BY). The use, distribution or reproduction in other forums is permitted, provided the original author(s) and the copyright owner(s) are credited and that the original publication in this journal is cited, in accordance with accepted academic practice. No use, distribution or reproduction is permitted which does not comply with these terms.